This article has been accepted for publication in a future issue of this journal, but has not been fully edited. Content may change prior to final publication. Citation information: DOI 10.1109/TUFFC.2020.3019932, IEEE Transactions on Ultrasonics, Ferroelectrics, and Frequency Control

Ultrasound for the Brain: A Review of Physical and Engineering Principles, and Clinical applications

Weibao Qiu, Ayache Bouakaz, Elisa E. Konofagou, Hairong Zheng

***Abstract*—The emergence of new ultrasound technologies has improved our understanding of the brain functions and offered new opportunities for the treatment of brain diseases. Ultrasound has become a valuable tool in preclinical animal and clinical studies as it not only provides information about the structure and function of brain tissues but can also be used as a therapy alternative for brain diseases. High-resolution cerebral flow images with high sensitivity can be acquired using novel functional ultrasound and super-resolution ultrasound imaging techniques. The non-invasive treatment of essential tremors has been clinically approved and it has been demonstrated that the ultrasound technology can revolutionize the currently existing treatment methods. Microbubble-mediated ultrasound can remotely open the blood brain barrier enabling targeted drug delivery in the brain. More recently, ultrasound neuromodulation received a great amount of attention due to its non-invasive and deep penetration features and potential therapeutic benefits. This review provides a thorough introduction to the current state-of-the-art research on brain ultrasound and also introduces basic knowledge of brain ultrasound including the acoustic properties of the brain/skull and engineering techniques for ultrasound. Ultrasound is expected to play an increasingly important role in the diagnosis and therapy of brain diseases.**

***Index Terms*—Brain ultrasound, Non-invasive brain imaging and therapy, High intensity focused ultrasound (HIFU), Low intensity focused ultrasound (LIFU).**

I. Introduction

Brain is the most complex and important organ in the human body. The advances in methodologies and tools for studying the brain often lead to the development of fundamental insights into the function of the brain. The emergence of new technologies and sophisticated tools, especially magnetic resonance imaging (MRI) and electroencephalograph (EEG) has dramatically accelerated our understanding of the human brain. However, MRI has a millimeter-level spatial resolution and only second-level temporal resolution, while EEG has a millisecond-level temporal resolution but centimeter-level spatial resolution. Novel methodologies and tools can provide great opportunities for the treatment of neurological and psychiatric disorders [1]. Nevertheless, there is still a shortage of treatment methods that are highly accurate and non-invasive.

Ultrasound has been used widely for diagnostic and therapeutic applications as it offers the advantages of non-invasiveness, fine resolution and safety [2, 3]. It has become a valuable tool in preclinical animal studies and clinical practice related to many areas of the brain. Brain ultrasound is a broad field that encompasses various techniques that use ultrasound waves to not only acquire real-time images of the brain tissue [4], but also treat brain diseases including cancer, cerebrovascular disease and neurological disorders [5, 6]. Ultrasound has limited applications for the brain unlike for other organs due to the challenges associated with penetrating through the skull [3].

Ultrasound imaging has been used frequently for evaluation of the cerebrovascular function of the brain as the ultrasound scanner is inexpensive, portable and can acquire images in real-time [7, 8]. Brain imaging using ultrasound has progressed recently thanks to the use of ultrafast Doppler for acquiring functional information of the brain [4]. This progress has created a breakthrough in the knowledge of brain research including brain hemodynamics, functional connectivity and cognitive neuroscience [9]. In addition, low frequency ultrasound can penetrate the brain skull, thus providing a highly promising tool for non-invasive brain therapy [10, 11]. Indeed, the ultrasonic energy can be concentrated in a small region of the brain, which permits a selective opening of the blood brain barrier (BBB) and, therefore, allows for the delivery of therapeutic drugs without systemic side effects [5].

Moreover, focused ultrasound (FUS) has received a significant amount of attention for non-invasive neuromodulation as it has been shown to be capable of modulating the neural activity in rodents[12-15], rabbits [16], pigs [17], sheep [18], non-human primates [19, 20] and humans [21]. Therefore, the FUS has become a highly promising tool for the treatment of brain diseases. Although there are many types of ultrasound equipment and methods that are being used for brain research and relevant clinical studies [6, 13, 22, 23], there are still several challenging niches that need to be overcome for brain imaging and therapeutics. The development

Manuscript received Mar 08, 2020. This work was supported by the National Key R&D Program of China (2018YFA0701400 and 2019YFC0121100), National Science Foundation Grants of China (81527901, 11874382 and 11534013), Shenzhen Research Grant (GJHZ20180420180920529, JCYJ20170413164936017, and ZDSYS201802061806314), Shenzhen Double Chain Project [2018]256, Youth Innovation Promotion Association CAS, CAS research projects (QYZDB-SSW-JSC018 and 2011DP173015), Natural Science Foundation of Guangdong Province (2014B030301013 and 2020B1111130002), and Guangdong Special Support Program.

W. Qiu and H. Zheng are with Shenzhen key laboratory of ultrasound imaging and therapy, Shenzhen 518055, China, and Paul C. Lauterbur Research Center for Biomedical Imaging, Shenzhen Institutes of Advanced Technology, Chinese Academy of Sciences, Shenzhen 518055, China.

Ayache Bouakaz is with UMR 1253, iBrain, Université de Tours, Inserm, Tours, France;

Elisa E. Konofagou is with the Department of Biomedical Engineering, Columbia University, New York, NY, US.

0885-3010 (c) 2020 IEEE. Personal use is permitted, but republication/redistribution requires IEEE permission. See http://www.ieee.org/publications_standards/publications/rights/index.html for more information.
Authorized licensed use limited to: Cornell University Library. Downloaded on September 01,2020 at 09:14:01 UTC from IEEE Xplore. Restrictions apply.

This article has been accepted for publication in a future issue of this journal, but has not been fully edited. Content may change prior to final publication. Citation information: DOI 10.1109/TUFFC.2020.3019932, IEEE Transactions on Ultrasonics, Ferroelectrics, and Frequency Control

of novel ultrasound methodologies and tools can provide great opportunities to facilitate the progress of brain research.

This review provides a summary of the state-of-the-art research progress on the applications of ultrasound for brain. It introduces basic knowledge including the acoustic properties of the brain/skull and the engineering techniques used in ultrasound. We provide a brief overview of the use of ultrasound for different brain applications, such as functional brain imaging, brain neuromodulation and brain therapy. This review addresses some of the most significant and recent contributions from the peer-reviewed published literature. In particular, the review gives the details of the methods including the waveform generation, skull distortion compensation, imaging techniques, treatment strategy, treatment monitoring, mechanism and safety issue. This review aims to provide a comprehensive knowledge of ultrasound technology for the brain.

II. Physical properties of brain and skull

A. Soft Brain Tissue

Brain is one of the most important organs, and its size varies significantly for different living species. Figure 1 shows the relative size of the brain of a mouse (~0.4 g, ~15.2 mm length*~8.9 mm width * ~5.6 mm height), rat (~1.9 g, ~22 mm length*~13 mm width * ~11 mm height), Rhesus monkey (~88 g, ~75 mm length * ~31 mm width * ~46 mm height), and human (~1500 g, ~167 mm length * ~140 mm width * ~93 mm height) [24-26]. These dimensions are approximate values in the largest cross-section because the brains are irregular spheroid shapes. The brain size is an important parameter for the ultrasonic focal point evaluation.

The acoustic properties of brain tissue are similar to those of other soft tissues in the human body. The density and speed of sound in brain tissues are about 1.03 g/cm^3 and 1550 m/s, respectively [27]. Therefore the acoustic impedance is about 1.6 MRayls. The speed of sound shows minor variations of less than 4 m/s over 1-5 MHz frequency, and increases to about 38 m/s when the temperature increases from 15 to 40 degrees [28]. The acoustic attenuation of the brain tissue is about 0.8 dB/cm*MHz [27], which decreases with increasing temperature, and the white matter has a higher attenuation compared to the gray matter [28]. The aforementioned values are representative and vary for different living subjects.

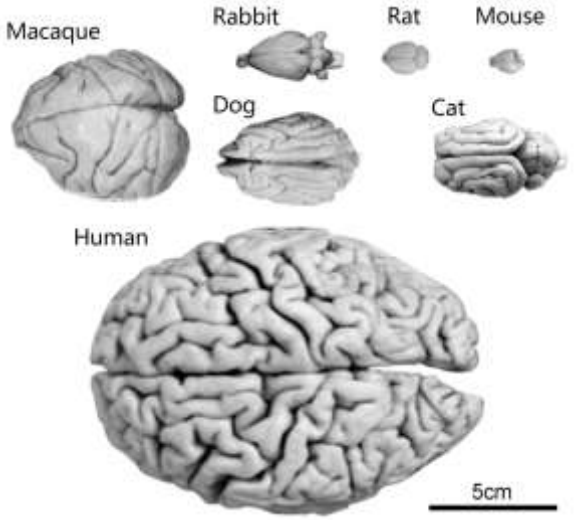

Fig. 1. Comparison of brain size of different species. Adapted from [26].

TABLE I
Acoustic properties of the human head.

Tissue	Speed of sound	Acoustic Impedance	Attenuation
Brain tissue	1550 m/s	1.6 MRayls	0.8 dB/cm*MHz
Skull	4080 m/s	7.75 MRayls	20 dB/cm*MHz
*Skin	1730 m/s	1.99 MRayls	3 dB/cm*MHz
Hair	-	-	Negligible when <0.5 MHz
Water	1480 m/s	1.48 MRayls	0.002 dB/cm*MHz

Note: The data are rough values and vary for different subjects and measurement settings. *The skin data are not from the scalp but shown here as a reference.

The brain tissue is protected by the skull bones, a covering of three thin membranes and the cerebrospinal fluid present inside the skull. The skin of the scalp is the thickest skin of the human body, and is up to 8 mm (normally 3-5mm) thick in adults [29]. The acoustic properties of the scalp are not available from the published literature. The density, speed of sound, and acoustic impedance of skin in other human parts are about 1.15 g/cm^3, 1730 m/s and 1.99 MRayls, respectively [27]. The acoustic attenuation of the skin tissue is about 3 dB/cm*MHz [30], which is relatively higher than that of other soft tissue. The acoustic properties of the tissues present in the human head are summarized in Table I.

The hair present on the patient's head is always a point of concern in clinical studies, and the current procedures require shaving the head before the ultrasound treatment. Existing research shows that the effect of the hair can be negligible when the ultrasound frequency is below 0.5 MHz [31, 32].

B. Skull Bone

The skull is a bony structure that provides a protective cavity for the brain tissues. It is comprised of many bones and the frontal, sphenoid, ethmoid, occipital, parietal and temporal bones are the most important ones when we deal with ultrasound propagation through the skull. These bones are shown in Fig. 2. Different bones are connected via sutures that are a type of fibrous joint. The thickness of the human skull varies significantly between different skull locations, as well as between different individuals. The thickness of the skull can range from 2 mm to 10.5 mm for adults, and increases gradually before the age of 20, and then stabilizes [33, 34]. As for the

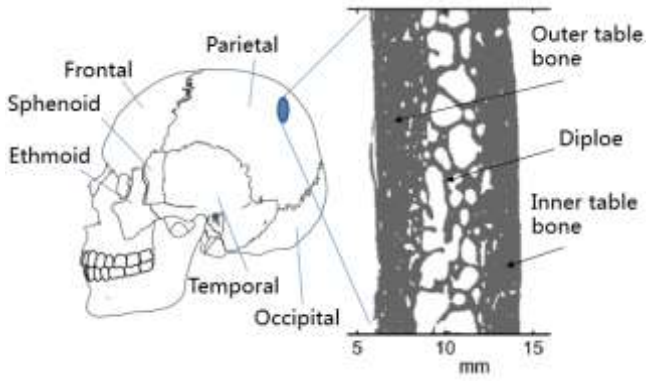

Fig. 2. The physical structure of the skull bone. The left side skull image is adapted from Wikipedia. Three-layer skull image is adapted from [35]. The temporal bone and occipital bone are the thinner areas of the human skull.

0885-3010 (c) 2020 IEEE. Personal use is permitted, but republication/redistribution requires IEEE permission. See http://www.ieee.org/publications_standards/publications/rights/index.html for more information.
Authorized licensed use limited to: Cornell University Library. Downloaded on September 01,2020 at 09:14:01 UTC from IEEE Xplore. Restrictions apply.

This article has been accepted for publication in a future issue of this journal, but has not been fully edited. Content may change prior to final publication. Citation information: DOI 10.1109/TUFFC.2020.3019932, IEEE Transactions on Ultrasonics, Ferroelectrics, and Frequency Control

temporal and occipital bones are the thinnest areas of the human skull so that they usually behave as acoustic windows [7]. Hence, these areas are usually exploited in transcranial ultrasound imaging for acquiring the flow information of the brain.

The acoustic property of the skull bone is different from that of the soft brain tissue. The skull has three parts: the outer table bone, the middle layer cancellous bone also known as the diploe, and the inner table bone [35]. The ultrasonic waves can interact with the complex microstructure of the cancellous bone present in the diploe layer. As the density of skull tissue is about 1.9 g/cm^3, and the speed of longitudinal waves is about 4080 m/s [27], the acoustic impedance is approximately equal to 7.75 MRayls, which is significantly higher than that of water or soft tissue.

The acoustic wave undergoes large attenuation losses due to acoustic reflection, scattering, absorption and mode conversion in the skull. The insertion loss through an intact human skull is highly dependent on the ultrasound frequency. In general, the one-way loss is about 10 dB and 20 dB at 0.5 MHz and 1.5MHz, respectively [36]. The acoustic attenuation caused by the skull tissue is about 20 dB/cm*MHz, which is significantly higher than that of human tissue [27].

The reflection at the skin-bone and bone-dura interfaces can be as high as 80% due to the high acoustic impedance mismatch between the tissues. The diploe layer has a lower acoustic impedance, and a large and highly frequency-dependent attenuation [36] because of its porous structure. Compared to the diploe layer, the outer and inner table layers have similar acoustic impedance and relatively low acoustic attenuation. The incident angle influences the ultrasound propagation. The conversion from longitudinal wave to shear wave in the skull is negligible when the incidence angle is less than 20 degrees [36].

C. Focal Beam in Brain

Focused ultrasound is important for imaging and therapy since the small size of the focal point increases the imaging resolution of living tissues and can be used for local treatment. Figure 3 shows the diagram of the ultrasonic focal beams and focal points. The focal points have the highest intensity in the acoustic field. The focal length for a focused transducer depends on the physical geometry, and the value in an array transducer can be adjusted using the phased delay of the array elements. The shape of the focal point is ellipsoidal and its size (-6 dB acoustic pressure at full width at half maximum) can be approximately calculated as follows [3]:

$$w = \lambda \times f_{number} = \lambda \times \frac{F}{D} \tag{1}$$

$$d = 7.2 \times \lambda \times f_{number} = 7.2 \times \lambda \times \left(\frac{F}{D}\right)^2 \tag{2}$$

where w is the width of the focal point, d is the length of focal point in the axial direction, λ is the ultrasound wavelength, and F and D are the focal length and effective aperture diameter of the transducer, respectively. Therefore, if large aperture transducers are used, the width and length of the focal point are approximately 0.5-3mm and 5-30 mm, respectively [3].

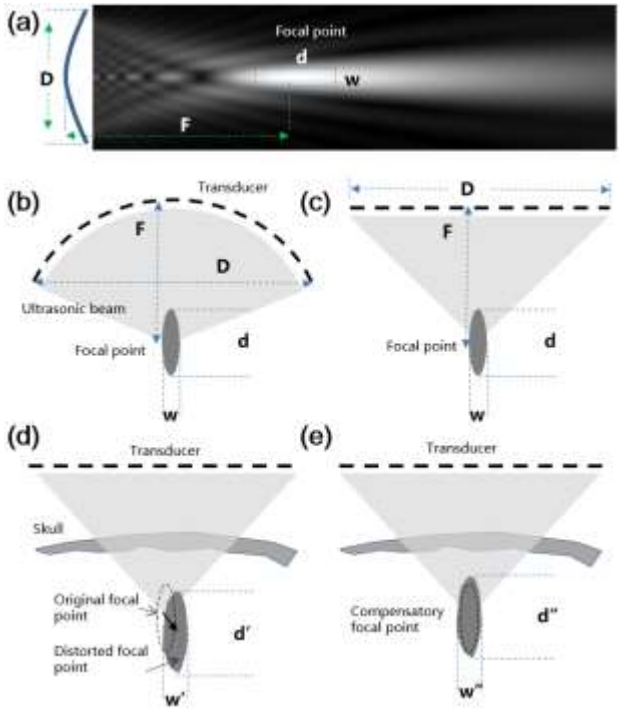

Fig. 3. Diagram of the focused ultrasound beams and focal points. (a) The acoustic field of a single element focused transducer with 1 MHz center frequency, 18 mm diameter, and 40 mm focal length. Simulated using Field II software. (b) Spherical focused transducer. (c) Flat array transducer. (d) The focal point is distorted because of skull bone, in which the size and position of focal point will change in the presence of the skull. (e) The skull distortion can be compensated using a phased array transducer.

D. Skull Measurement and Compensation

One major issue encountered by brain ultrasound in a clinical study is the distortion effects caused by the skull bone, which include attenuation, aberration, refraction and mode conversion. Therefore, the ultrasonic waveforms are distorted when the ultrasound waves pass through the skull as shown in Fig. 3d. The position of the focal point may shift and the -6 dB area may increase unevenly. The use of ultrasound is still acceptable in some applications such as transcranial Doppler (TCD) flow imaging even though a single element transducer is used and the focal point is distorted. The performance of brain ultrasound can improve significantly if the aforementioned distortions in the skull can be minimized.

Using an array transducer for skull compensation is an established method for reshaping the focal point. In this method, the array transducer is combined with a dedicated beamformer to adjust the wave-front and correct for the skull phase aberrations, such that a precise and focused beam is generated at the target after propagation through the skull. An array transducer with different adaptively phased ultrasound waves emitted from each array element is widely used to correct the distortions due to the skull [3, 37]. The focal point can be reshaped by phase realignment if the speed of sound and thickness of the incident position of the skull can be acquired precisely, as shown in Figs. 4b-c. Therefore, it is important to know the thickness and the speed of sound through the skull for ultrasound compensation.

There are several methods proposed for characterizing the skull using computed tomography (CT) [38], magnetic resonance imaging (MRI) [39] and ultrasound backscatter [40].

0885-3010 (c) 2020 IEEE. Personal use is permitted, but republication/redistribution requires IEEE permission. See http://www.ieee.org/publications_standards/publications/rights/index.html for more information.
Authorized licensed use limited to: Cornell University Library. Downloaded on September 01,2020 at 09:14:01 UTC from IEEE Xplore. Restrictions apply.

This article has been accepted for publication in a future issue of this journal, but has not been fully edited. Content may change prior to final publication. Citation information: DOI 10.1109/TUFFC.2020.3019932, IEEE Transactions on Ultrasonics, Ferroelectrics, and Frequency Control

Currently, the CT-based skull compensation method is used in clinical studies although ionized radiation is involved in CT scanning. First, high-resolution multiple slices CT images can be acquired, and then the thickness of skull bone can be obtained directly from the CT image. The speed of sound and porosity map of the skull are interrelated. The porosity of the skull Φ can be calculated as

$$\Phi=1-\frac{HU}{1000} \tag{3}$$

where *HU* represents the CT Hounsfield units indicating the absorption of tissue in the X-ray. The values of *HU* range from 0 (for water, assuming no air in the skull) to ~1700 (typical cortical bone), as shown in Fig. 4a.

Subsequently, the density ρ , the speed of ultrasound *c*, and the absorption α can be obtained as follows [38]:

$$\rho=\Phi\times\rho_{water}+(1-\Phi)\times\rho_{skull,\max} \tag{4}$$

$$c=\Phi\times c_{water}+(1-\Phi)\times c_{skull,\max} \tag{5}$$

$$\alpha=\alpha_{water}+\Phi^{\gamma}\times(\alpha_{skull,\max}-\alpha_{water}) \tag{6}$$

where ρ_{water} is the mass density of water, and $\rho_{skull,\max}$ is the maximum density in cortical bone. The speed of ultrasound in water and the maximum speed of ultrasound in cortical bone are represented by c_{water} and $c_{skull,\max}$, respectively. Similarly, the ultrasound absorption of water and the maximum absorption of the skull are denoted by α_{water} and $\alpha_{skull,\max}$, respectively. The values of γ can vary from 0.3 to 0.7 [38], which represents varying absorption of wave fronts propagating through different skull parts. Finally, the waveform can be compensated using the estimated thickness, density, speed of sound, and absorption coefficient.

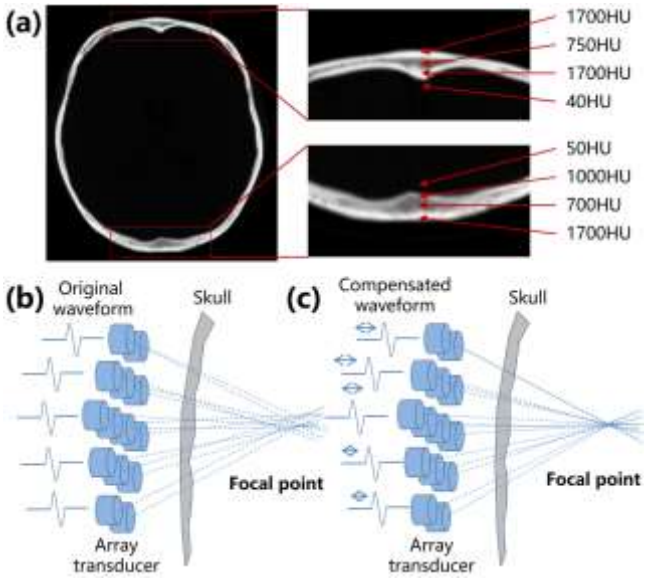

Fig. 4. (a) The CT image of a human skull. Typical values of Hounsfield units have been labeled. (b) Waveform distortion induced by the skull bone. (c) The compensated waveform after the skull bone and the focal point was reshaped to a normal state.

The CT-based aberration correction suffers from a few limitations mainly in the presence of micro-porosities that cannot be detected by clinical CT due to its low resolution. Micro-porosity in the skull affects attenuation and can vary across patients or even across a skull of the same patient. In addition to the CT-based method, MRI and ultrasound imaging have also been proposed for characterizing the skull. Ultrashort echo-time MRI was applied to acquire the weak and short-lived signal from the skull bone and correct the ultrasound aberration induced by the skull [39].

It was reported in the literature that there was no significant difference using the CT-based and MR-based correction method when the corresponding data were imported in the aberration correction software provided by the manufacturer (Exablate Neuro, Insightec). In addition, ultrasound itself can be used for skull characterization using focused ultrasonic waves. The front and back ends of the skull can be acquired by moving the focal point across it, and subsequently, the thickness and speed of sound in the skull bone can be calculated [40, 41]. The dual transducers method was proposed to correct the wave-fronts and obtain a high level of focusing inside the skull [42]. However, more data and *in vivo* results are required to demonstrate the feasibility of MRI or ultrasound-based compensation methods.

III. Ultrasound Imaging for the Brain

A. Transcranial Ultrasound Imaging

Transcranial ultrasound is a noninvasive, nonionizing, inexpensive, portable and real-time imaging modality. It has been used frequently for cerebrovascular function evaluation [7]. Even though the skull bone causes the ultrasound beam to attenuate and distort significantly, the imaging of the brain can still be carried out through the relatively thinner skull bones. Two skull windows are present in the temporal bone near the ear and the occipital bone in the back. Both of these bones are thin and as a result, the skull aberrations are minimal in these two skull regions compared to other parts of the skull. Transcranial ultrasound imaging usually utilizes the ultrasound frequencies within the 1.5 to 2.5 MHz range to achieve a balance between ultrasound imaging resolution and skull attenuation. Higher frequencies undergo severe attenuation and distortion, and low frequency provides low resolution. However, 5% of brain imaging results are not successful because the ultrasound waves cannot penetrate the temporal bone sufficiently to allow analysis of intracranial hemodynamics [43].

Transcranial ultrasound imaging includes a single element transducer-based transcranial Doppler (TCD) and array-based transcranial color Doppler (TCCD). Both modes exploit the temporal and occipital bones as acoustic windows to acquire the flow information of the brain. The TCD has a single element narrow bandwidth and high sensitivity transducer with 1.5-2.5MHz center frequency, ~8 mm diameter and ~60 mm focal length. The transducer is used to acquire the pulsed Doppler shift frequency induced by the blood flow in the cerebral vessel. Figures 5a-b show the setup for brain imaging using a TCD probe (Shenzhen Delica Electronics Co., Ltd,

0885-3010 (c) 2020 IEEE. Personal use is permitted, but republication/redistribution requires IEEE permission. See http://www.ieee.org/publications_standards/publications/rights/index.html for more information.
Authorized licensed use limited to: Cornell University Library. Downloaded on September 01,2020 at 09:14:01 UTC from IEEE Xplore. Restrictions apply.

This article has been accepted for publication in a future issue of this journal, but has not been fully edited. Content may change prior to final publication. Citation information: DOI 10.1109/TUFFC.2020.3019932, IEEE Transactions on Ultrasonics, Ferroelectrics, and Frequency Control

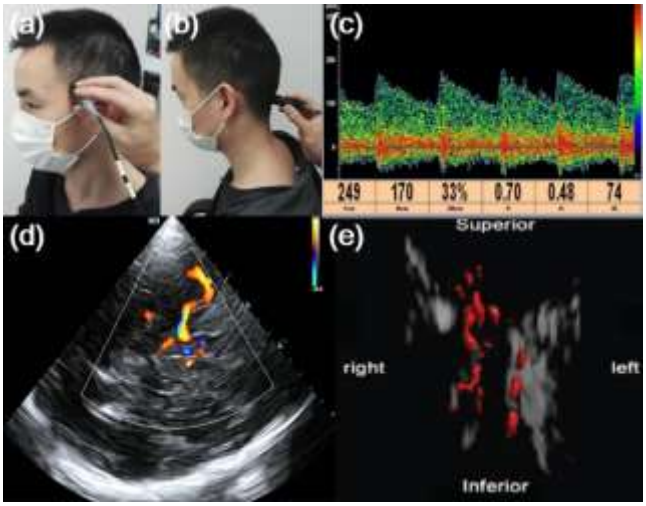

Fig. 5. Transcranial ultrasound imaging method and clinical images. The acquisition position of a TCD probe through (a) temporal window and (b) occipital window. (c) Pulsed wave Doppler imaging in the human brain. The images are provided by Delica. (d) Color Doppler image of the blood flow of the middle cerebral artery. The image is provided by Mindray. (e) The 3D cerebral flow ultrasound imaging. The image is from [45].

Shenzhen, China) through the temporal or occipital window, and Fig. 5c shows the Doppler spectrum display of the middle cerebral artery. The TCD has been applied for identifying cerebrovascular diseases such as acute stroke, intracranial arterial stenosis and occlusion, vasospasm, subarachnoid hemorrhage and sickle cell disease [7].

Transcranial color Doppler (TCCD) can visualize the blood flow of the anterior cerebral artery, middle cerebral artery and posterior cerebral artery for the auxiliary diagnosis of stroke. Figure 5d shows the image of the blood flow in the middle cerebral artery image (acquired by M9, Shenzhen Mindray Bio-Medical Electronics Co., Ltd), which can be utilized for the diagnosis of emboli, stenosis and other pathologies. The TCCD typically uses a phased array transducer with 1.5-2.5MHz center frequency and an aperture size that can fit within the acoustic window. The technical specifications of the array transducer for brain imaging match closely with those of the transducer for transthoracic echocardiography [44]. Contrast-enhanced ultrasound imaging using microbubble can be useful in assessing real-time cerebral perfusion changes [8]. In addition, transcranial 3D ultrasound volume imaging was realized using a 2D array transducer [44-47].

Although several reports have been published on the topic of skull effect compensation for brain imaging [40-42, 48, 49], there is only limited work available using clinical ultrasound scanner [46, 47]. There is an increasing need for improving the image quality of brain ultrasound imaging. Super-resolution ultrasound brain imaging was proposed to improve the resolution and accuracy of brain vascular mapping and an *ex vivo* study was carried out using the human skull [50, 51]. Acoustic metamaterials [52] and time-reversal [53] may improve the imaging quality but there are no data available till now.

Nonetheless, as the skull effect is minimal for neonates, high-frequency ultrasound (~7MHz) has been used for transcranial ultrasound imaging through the fontanelle window [9, 54] to detect abnormalities in their brains. Ultrasound Doppler imaging can non-invasively image the spatial and temporal dynamics of microvascular changes that can occur during seizures and interictal periods with a very high resolution at bedside [9].

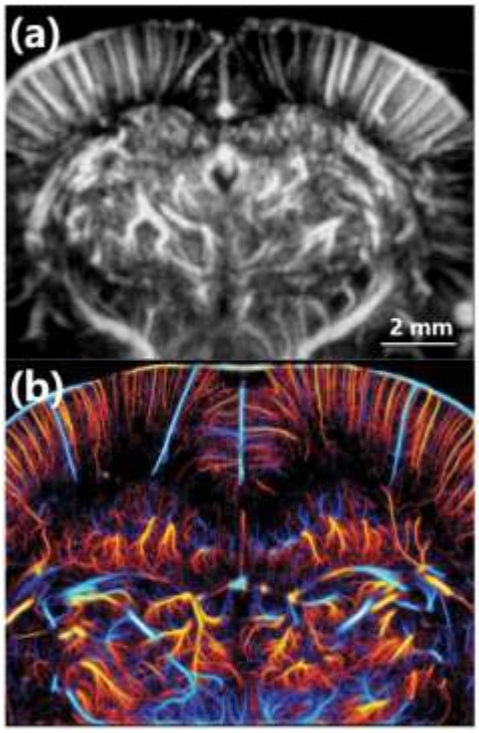

Fig. 6. Cerebral flow images of rodent in the absence of skull using (a) plane-wave based functional ultrasound [57], and (b) super-resolution ultrasound, adapted from [61].

B. Ultrasound Imaging in the Absence of Skull

Open skull surgery, also known as craniotomy is usually performed to treat brain tumors, aneurysms, hematomas, and traumatic head injury. In this surgery, a part of the skull bone is removed to expose the brain tissues. Therefore, ultrasound imaging can be easily carried out in the absence of skull [55, 56], with the ultrasound frequency in the range of 5-15MHz. Contrast-enhanced ultrasound is highly useful for improving the delineation between the tumor and healthy tissue pre-resection, as well as for showing the remaining tumor tissues after the initial resection [55].

The recently proposed plane-wave based power Doppler ultrasound imaging method has been applied for cerebral flow imaging. In this method, parallel ultrasonic data were transmitted and received by all the array elements synchronously unlike the conventional line-by-line scanning [2]. Usually, a three-cycle pulse was employed and very high frame rate data were acquired to increase Doppler ultrasound sensitivity for imaging the blood flows in small cerebral vessels [4]. The flow data can be quantified to evaluate brain tumors (as shown in Fig. 6a) [57], which may help to precisely assess the brain tumors characteristics before or during surgical resection.

The several advantages of ultrasound make it a unique tool to acquire information of brain functions and allow tracking the spatiotemporal dynamics of the brain activities [4]. Ultrasound was also shown to be sensitive enough to map the functional connectivity in a living rat's brain with a significantly higher spatiotemporal resolution than fMRI. Therefore, the brain ultrasound imaging method is usually referred to as the

0885-3010 (c) 2020 IEEE. Personal use is permitted, but republication/redistribution requires IEEE permission. See http://www.ieee.org/publications_standards/publications/rights/index.html for more information.
Authorized licensed use limited to: Cornell University Library. Downloaded on September 01,2020 at 09:14:01 UTC from IEEE Xplore. Restrictions apply.

This article has been accepted for publication in a future issue of this journal, but has not been fully edited. Content may change prior to final publication. Citation information: DOI 10.1109/TUFFC.2020.3019932, IEEE Transactions on Ultrasonics, Ferroelectrics, and Frequency Control

functional ultrasound (fUS) [4]. The fUS can assess local changes in cerebral blood volume that can occur during cognitive tasks. Its temporal resolution is high enough to measure the directional propagation of signals [58]. It has also been used concurrently with extracellular recordings of local field potentials to reveal brain-wide spatiotemporal hemodynamics of single rapid eye movement sleep episodes [59].

More recently, with the introduction of super-resolution imaging for the brain applications, the ultrasound modality has achieved a major breakthrough [60]. It uses individually localized microbubbles that have a resolution of less than 20 μm. The positions of the moving microbubbles are tracked and accumulated to generate a super-resolution image, shown in Fig. 6b. The generation of this image overcomes the diffraction-limit of spatial resolution [61]. This novel neuroimaging modality based on ultrafast ultrasound provides new insights into the brain dynamics and neuroscience studies.

IV. Ultrasonic therapy for brain

Ultrasound can be focused in a small area in the human brain allowing for precise, incisionless, transcranial delivery of acoustic energy into the brain tissue. In this section, two focused ultrasound methods and their applications are presented, including high intensity focused ultrasound (HIFU) and low intensity focused ultrasound (LIFU). The former produces tissue ablation, while the latter is a non-destructive treatment, during which the tissue is safe and intact. The acoustic properties of therapeutic ultrasound for the brain are summarized in Table II.

TABLE II
Typical acoustic properties of therapeutic ultrasound for the brain.

Technique	Frequency	Waveform	Power	Stage
HIFU Ablation	0.5-0.8MHz	10-25s Continuous waveform	150-950 W	Clinical
Histotripsy Ablation	0.3-1.5MHz	Short pulse, ~2 cycles or ~1% PRF	High pressure ⩾ 30MPa	Preclinical
BBB opening	0.2-1.5MHz	Short pulse, ~1% low PRF	Low pressure ~0.5 MPa	Clinical trial
Neuro-modulation	0.2-5MHz	Low PRF pulse or shock wave	Low pressure or short high pressure	Preclinical and clinical trial
Sonothrom-bolysis	0.3-2MHz	Low PRF short pulse	Low pressure	Clinical trial

A. Ablation of Brain Tissue

The HIFU allows the ablation of a precise volume of tumor tissues by generating peak temperatures ranging from 51 to 60 degrees Celsius without any side effects or neurological deficits [62]. Generally, focused ultrasound with 10-25 seconds duration, 0.5-0.8 MHz center frequency and 150-950 Watt acoustic power was transmitted into the brain tumor, where the acoustic attenuation converted acoustic energy into heat [63].

It has been demonstrated that using ultrasound to treat malignant glioma [63] and various functional brain diseases including chronic neuropathic pain [64], essential tremor [65], and Parkinson's disease [66] through thermal ablation of thalamic and subthalamic targets is both feasible and safe. Ultrasound brain therapy offers a reduced risk of damage to the non-targeted areas, and blood clot formation compared to the traditional RF ablation [67] or deep brain stimulation (DBS). It is performed while the patient is awake and does not involve any anesthesia, scalp incisions, burr holes through the skull or insertion of electrodes into the brain. It is a non-invasive, single treatment approach that enables the patients to recover rapidly.

Ultrasound undergoes high attenuation through the skull bone and, therefore, the heat generated in the skull bone cannot be ignored. A three to five minute break must be applied after a 10–25-second sonication to allow the skull bone and adjacent tissue to cool down and prevent adverse thermal lesions [63]. Another limitation of the existing brain HIFU methods is that the therapeutic target is located around the central part of the brain. Moreover, the treatment volume should be monitored to prevent overheating of the skull even when the target is located in the central portion of the brain. Overheating may occur for large treatment volumes. Currently, a variety of methods to broaden the treatment area are being evaluated, including using lower frequency ultrasound [68, 69], ultrasonic microbubble mediated therapy [70] and new transducer arrangement [71, 72]. A new method for brain HIFU can enhance the therapeutic potential of ultrasound for various brain diseases in the future.

In addition to the thermal ablation, histotripsy is another therapeutic method for the brain [73, 74]. In this method, the pulse duration is usually short: microsecond for histotripsy and millisecond for boiling histotripsy. The pulses have very high acoustic pressures (⩾30MPa), and the ultrasonic frequency is in the range of 0.3-1.5MHz. Bubble clouds are generated within the tissues and ablation is induced by the rapid collapse of the bubbles. Furthermore, highly localized mechanical stress and strain liquefy the target tissue into acellular debris. Histotripsy has been demonstrated to generate sharply defined lesions of arbitrary shapes and sizes in the swine cortex [75]. The latest developments in random phased array and nonlinear trans-skull focusing technology for boiling histotripsy have the potential to create shocks with aberration correction at points located inside the skull [76, 77].

B. Blood-brain-barrier (BBB) Opening Therapy

The BBB is a complex structure that protects the brain from exposure to potentially damaging substances. However, it also blocks the therapeutic drugs used for treating neurodegenerative and oncological diseases. Microbubble-mediated LIFU has been demonstrated to be feasible and safe for targeted delivery of drugs through transient permeabilization of BBB. The delivered drugs can be used to treat brain diseases including Alzheimer's disease (AD) [5], brain tumors [78], myotrophic lateral sclerosis [6] and other diseases of the central nervous system. These studies show that ultrasound can become an option to treat many neurological disorders, as the technology can be used to safely open the BBB and deliver therapeutic agents to the brain.

The sonication targets have a size of 5 mm × 5 mm × 7mm in the brain. They can be treated using a 0.22 MHz ultrasound [6], and the frequency can vary over a large range from 0.2 to 1.5 MHz or higher. The acoustic pressures should be higher than

0885-3010 (c) 2020 IEEE. Personal use is permitted, but republication/redistribution requires IEEE permission. See http://www.ieee.org/publications_standards/publications/rights/index.html for more information.
Authorized licensed use limited to: Cornell University Library. Downloaded on September 01,2020 at 09:14:01 UTC from IEEE Xplore. Restrictions apply.

This article has been accepted for publication in a future issue of this journal, but has not been fully edited. Content may change prior to final publication. Citation information: DOI 10.1109/TUFFC.2020.3019932, IEEE Transactions on Ultrasonics, Ferroelectrics, and Frequency Control

0.3 MPa [79]. Ultrasound is usually delivered in a burst mode, and each spot sonication consists of typically 2 ms on and 28 ms off bursts for 300 ms, with a repetition interval of 2.7 s for human study [5]. A sonication cycle is between 50-90 s and one to two sonication cycles can be applied until the BBB opens [6]. Each sonication cycle is coupled with a weight-based intravenous injection of 4 μl/kg microbubbles, followed shortly by the application of ultrasound to the target. The total dose of the injection should not exceed 20 μl/kg [5, 6]. Several commercially available microbubbles (Sonovue, Bracco Diagnostics Inc., Milan, Italy; Definity, Lantheus Medical Imaging, USA) are suitable for BBB opening studies. It is reported that the BBB can be closed within 24 hours or less using appropriate settings [79].

C. Ultrasound Neuromodulation

Neuromodulation is a technique that has been used for basic and clinical neurosciences. It applies electrical, magnetic, optical, acoustic, and/or pharmaceutical agents to neurons for altering their activity. Neuromodulation based on the LIFU is an emerging technique that can non-invasively modulate the neural activities in the brain by delivering low-intensity ultrasonic waves through the intact skull [21]. Compared to other neuromodulation approaches, the LIFU-based approach is non-invasive and can reach deep brain regions with a high spatial resolution of about several millimeters. Thus, it has attracted a significant amount of attention in the field of brain science [80].

The parameters of the ultrasound wave for ultrasound neuromodulation are similar to those required for BBB opening. The frequency range can be very large in the range of 0.2MHz-43MHz [80, 81]. Usually, low frequency ultrasound, i.e., less than 2.5 MHz is used for stimulation because the penetration depth is high for low frequency ultrasound. The width of the focal point in a small animal's brain can be less than 1 mm when a 5MHz ultrasound is used [12]. The parameters of sonication vary for different experiments. A successful activation can be induced for acoustic pressure values that are usually higher than a threshold of 0.3 MPa [12]. The LIFU is normally delivered in a burst mode to avoid a temperature increase [82]. Each spot sonication typically has a duty factor of 50%, consisting of about 1 ms on and 1 ms off bursts for 2-300 ms, with a repetition interval of 2-3 s [15]. The number of sonication cycles depends on the study: transient stimulation can be achieved in one cycle, and long term treatment may require treatment cycles each time of several minute.

Another method uses a very short but very high acoustic pressure ultrasonic wave for neuromodulation. The wave duration is about 3 μs, the positive and negative pressures are 20 MPa and 10 MPa, respectively, the energy flux density is 0.2-0.3 mJ/mm^2 and the pulse repetition frequency is 1-5 Hz. This method was applied for treating Alzheimer's disease patients, whose neuropsychological scores improved immediately as well as one and three months after the ultrasound stimulation [83].

The LIFU was applied to modulate the connectivity profiles of the brain, which indicated that such stimulation could selectively target structures deep in the macaque brain [84]. In addition, ultrasound increased the functional coupling of the stimulated regions with the strongly or closely connected regions [20]. A further understanding of the potential mechanisms is necessary for better application of ultrasound in brain neuromodulation. The LIFU can be a highly useful tool for modulating specific neuronal pathways or nuclei in both clinical and basic neuroscience studies such as aging [85] and social behavior. The latest development of portable devices and systems for studying awake animals provides new options for ultrasound neuromodulation [13, 15, 86]. In addition to a general neuromodulation tool, the LIFU has demonstrated its potential therapeutic effects on neurologic diseases including Parkinson's disease [87], depression [88], and epilepsy [89-91] in small animals. Moreover, ultrasound neuromodulation can be developed as a general noninvasive sonogenetic method to manipulate the neural activities [92].

D. Sonothrombolysis

Early recanalization of patients with acute ischemic stroke can significantly reduce the disability rate. However, a large number of stroke patients remain disabled after the interventional treatment using tissue plasminogen activator (t-PA). The LIFU has been aided by using t-PA, known as sonothrombolysis to treat acute ischemic stroke. It was found that the LIFU (2MHz pulsed transcranial ultrasound) can induce a detectable improvement of residual flow and early recanalization with the t-PA therapy [93]. In addition, the LIFU having the same diagnostic settings as those used originally for the TCCD with a 2 MHz transducer through the temporal bone has been evaluated. Microbubble mediated sonothrombolysis may augment recanalization therapy for acute ischemic stroke [94]. However, another clinical trial using low frequency ultrasound at 0.3MHz for sonothrombolysis was stopped due to an increased rate of cerebral hemorrhages in patients caused after the tPA treatment [95]. There is a risk of brain damage during tPA extravasation due to inertial cavitation and standing wave hurdles in low frequency ultrasound [96].

E. Imaging Guidance for the Therapy

Currently, MRI has been employed for real-time guidance of ultrasound brain therapy [3]. The MRI can provide a good contrast between soft tissues and skull, and is sensitive to subtle changes in morphology and functions. Therefore, MRI can be used to monitor the focal point by providing visualization of the temperature elevation and displacement induced by the focused ultrasound, which in turn can be used to localize the position of therapy. A variety of MRI parameters are sensitive to the thermal effects induced by ultrasound, among which the protons resonance frequency is the most widely used parameter for monitoring the ultrasound therapy [97]. The resonance frequency of proton in water molecules demonstrates a linear relationship with the temperature change. A relatively low power ultrasound of about 150 to 250 W induced temperatures of 40 to 45 ℃ and resulted in confirmed accurate focusing in the brain using the MR thermography [65]. The temperature was continuously monitored during the therapeutic procedure, which ensured the safety and reliability of ultrasound therapy for noninvasive brain neurosurgery.

The MR acoustic radiation force imaging (MR-ARFI) [98] is another method to guide the ultrasound treatment. The micro-scale local displacement induced by the ultrasound

0885-3010 (c) 2020 IEEE. Personal use is permitted, but republication/redistribution requires IEEE permission. See http://www.ieee.org/publications_standards/publications/rights/index.html for more information.
Authorized licensed use limited to: Cornell University Library. Downloaded on September 01,2020 at 09:14:01 UTC from IEEE Xplore. Restrictions apply.

This article has been accepted for publication in a future issue of this journal, but has not been fully edited. Content may change prior to final publication. Citation information: DOI 10.1109/TUFFC.2020.3019932, IEEE Transactions on Ultrasonics, Ferroelectrics, and Frequency Control

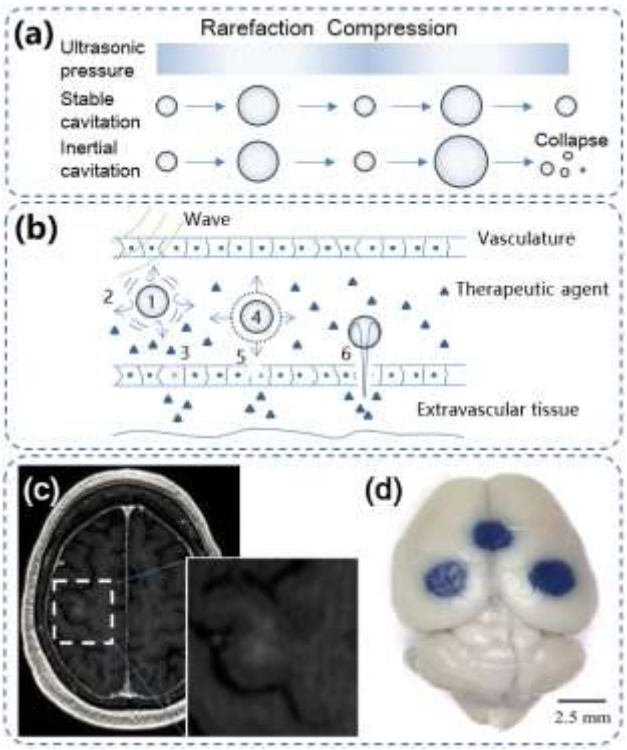

Fig. 7. (a) Stable and inertial cavitation of microbubble induced by ultrasonic wave. The image is adapted from [111]. (b) Bioeffect of acoustic micro-bubble in the vessel: 1. Stable cavitation; 2. microstreaming around the bubble; 3. Non-ruptured permeability; 4. Shock wave causing by collapse cavitation; 5. Pierced and ruptured cell; 6. A liquid jet that pierces the endothelial lining. The image is adapted from [111]. (c) MRI images of brain tissue when BBB is open. The image is adapted from [6]. (d) Evans blue extravasation in brain tissue indicating multiple BBB opening positions. The image is from [106].

insonation can be encoded as the phase contrast. As the ultrasound pulses with a low duty cycle have minor thermal effects, they can be used to monitor nonthermal treatment such as target drug delivery, BBB opening, and neuromodulation. Adaptive algorithms based on the MR-ARFI feedback that can correct phase aberrations caused by the skull were reported in [99, 100]. However, a high ultrasound intensity was required to obtain good quality transcranial images. A simultaneous MR-ARFI thermometry sequence with high temporal and spatial resolution was proposed for sub-second multi-slice temperature and displacement imaging during sonication [101].

All the aforementioned methods help in better targeting of the brain structures with improved safety profile and therapy efficiency. Once the focal point and the ultrasonic intensity are verified and confirmed, the MRI can also be used to monitor the process of BBB permeabilization in the brain using new gadolinium enhancement in T1-weighted imaging [6], as shown in Fig. 7c. The visualization of gadolinium enhancement in the brain target effectively shows the BBB opening, thus indicating when the sonication procedure should be terminated [6].

In terms of microbubble mediated therapy applications, harmonic and ultra-harmonic acoustic feedback from the targeted area can be used to indicate the level [6] and location of cavitation [102-104]. In addition, Evans blue extravasation is frequently used for small animal studies [105, 106], where the blue color indicates the permeabilization area in the brain tissue, as shown in Fig. 7d.

TABLE III
MECHANISM OF ULTRASOUND FOR BRAIN IMAGING AND THERAPY.

Applications	Mechanism
B-mode imaging	Mechanical wave effect
Doppler imaging	Mechanical wave effect, Doppler effect
Contrast mode imaging	Mechanical wave effect, non-linear ultrasound, cavitation effect
Elasticity imaging	Mechanical wave effect, acoustic radiation force, shear wave propagation
Ablation	Thermal effect, cavitation effect [108]
BBB opening	Cavitation effect, sonoporation, acoustic radiation force, microstreaming [110-112]
Neuromodulation	Potentials piezoelectric effect, intramembrane cavitation, acoustic radiation force, cavitation effect [81, 109, 113, 115-6]
Thrombolysis	Cavitation effect, acoustic radiation force, thermal effect [117]

Furthermore, 3D infrared camera technology can also be used to guide the therapy [23, 83]. An optical sensor is attached to the transducer and, therefore, the 3D position of the sensor is known and the focal point of the transducer can be tracked simultaneously. Consequently, the ultrasonic focus can be simulated in real-time in the brain map that is acquired a priori by CT or MRI scanner. This method removes the need of ultrasound equipment for MRI compatible issues and simplifies the therapeutic process. However, the skull aberrations cannot be compensated because of the low resolution of the guidance technology, which is about 1-2mm.

V. MECHANISM

Ultrasound are mechanical waves that can travel through the living tissue. The interactions of ultrasound with the living tissues are complex and, therefore the mechanism behind the interactions is also complex and sometimes involves several factors. The mechanism in play differs depending on the therapeutic applications, as summarized in Table III.

A. Imaging

Ultrasound interacts with the living tissues when traveling through them. These interactions can include reflection, scattering and absorption. The reflection occurs when the ultrasound waves encounter difference in acoustic impedance. The transducer composes an image from the received reflected signal, which represents the relative variations of acoustic impedance in living tissues. This is known as B-mode imaging. The microbubbles used as contrast agents in clinical studies are micron-sized and, therefore they can be easily introduced intravenously. The bubbles are typically gas-filled bodies that significantly increase the scattering of ultrasound waves, especially the nonlinear scattering. As a result, they can be easily differentiated from soft tissue structures, which is known as Contrast mode. A change in the frequency of an ultrasound wave, known as the Doppler effect, is caused by the blood flow. This frequency change can be used to detect the velocity and

0885-3010 (c) 2020 IEEE. Personal use is permitted, but republication/redistribution requires IEEE permission. See http://www.ieee.org/publications_standards/publications/rights/index.html for more information.
Authorized licensed use limited to: Cornell University Library. Downloaded on September 01,2020 at 09:14:01 UTC from IEEE Xplore. Restrictions apply.

This article has been accepted for publication in a future issue of this journal, but has not been fully edited. Content may change prior to final publication. Citation information: DOI 10.1109/TUFFC.2020.3019932, IEEE Transactions on Ultrasonics, Ferroelectrics, and Frequency Control

direction of the blood flow. This is known as Pulse-wave Doppler and Color Doppler mode [107].

B. Therapy

The absorption of ultrasound waves in tissues causes thermal effects that have been exploited for the HIFU thermal ablation applications. A therapeutic sonication of 10 to 20 seconds can induce a temperature increase of the targeted tissue from 40 to 63℃ for the maximal voxel monitoring using MR thermography [65]. In addition, inertial cavitation may occur due to high mechanical indices that can generate high temperature and pressure elevation within proximity to the targeted tissue, which contributes further to the thermal ablation [108].

The permeabilization of BBB requires microbubble mediated ultrasound and multiple physical phenomena can play a role in this process as shown in Fig. 7a-b. The microbubbles oscillate at low-pressure ultrasound waves, which is known as stable cavitation, The resulting oscillations can interact with the vascular lining [109]. In addition, rapid oscillation may create micro-streaming, which in turn may interact further with the vascular lining creating high shear stress. The acoustic radiation force can also contribute to this cascade process by pushing the bubbles. The bubbles may collapse when high acoustic pressure is applied, and the accompanying shock wave and micro-jet can induce vascular permeabilization [110, 111].

The mechanism behind ultrasound neuromodulation is still not fully understood, although several studies have been carried out in recent years. The process may involve multiple physical phenomena including mechanical waves, piezoelectric effects, acoustic radiation force, cavitation, and/or thermal effects.

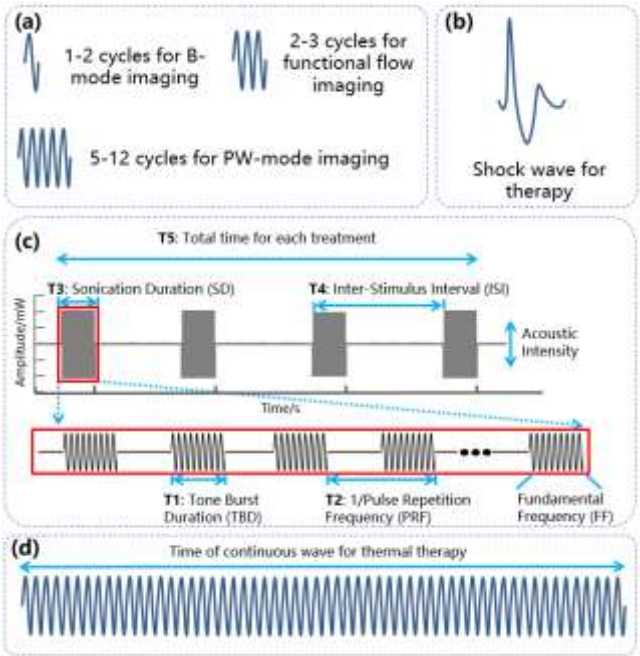

Fig. 8. Acoustic waveforms for ultrasound applications. (a) One cycle pulse is for B-mode imaging, and 2-3 cycle for functional ultrasound imaging. More than 5 cycles for Doppler imaging. (b) High-pressure shock wave for histotripsy and neuromodulation. (c) The pulsed waveform for LIFU application. T_1 is the continuous pulse duration; T_2 is the pulse repetition period; T_3 is the sonication duration; T_4 is the stimulus repetition period; T_5 is the total time for each treatment. (d) Continuous-wave (>20 seconds) for thermal ablation.

Mechanosensitive channel may be a factor that causes ultrasound neuromodulation [112, 113]. A mechanosensitive channel of large conductance (MscL) was found in rat hippocampal neurons in primary culture, which could be activated by ultrasound [112]. Piezo-type mechanosensitive ion channel component 1 (Piezo1) mediates the *in vitro* action of mouse primary cortical neurons and can also be activated by ultrasound [113]. In addition, the acoustic radiation force was deemed as a physical mechanism behind neuronal cell stimulation [81]. A hypothesis was proposed according to which the neuronal intramembrane piezoelectricity was responsible for causing ultrasound neuromodulation [114]. The capacitance of the intramembrane changed due to the conformational state of the lipids in the membrane, which generated a nerve impulse [115]. However, all these aspects require confirmation using further experimental data, and the underlying mechanism can be more complex than a single physical phenomenon.

Cavitation has been hypothesized as the main source of thrombolysis. Stable cavitation in the vicinity of blood clots facilitates the efficacy of lytic drugs and inertial cavitation produces micro-jet that can further cause physical damage to the blood clot's surface [116]. In addition to cavitation, acoustic radiation force could be responsible for sonothrombolysis [117].

VI. Safety

The safety of brain ultrasound depends on the mechanical and/or thermal effects of ultrasound. The mechanical effect is mainly induced by acoustic radiation force or acoustic cavitation. It can damage the normal cell structure and cause bleeding in the capillary around the targeted tissue. The thermal effect can increase brain tissue temperature resulting in protein denaturation or cell death.

Figure 8 shows a typical ultrasonic waveform for brain ultrasound applications. A good imaging resolution should be obtained for structural imaging, and therefore, the pulse should be as short as possible, usually between one to three cycles. One-cycle pulse can provide the best imaging resolution. Two-cycle will increase the echo amplitude at the expense of imaging resolution. Typically, a three-cycle waveform was used for functional ultrasound flow imaging and a 5-10 cycle waveform was used for pulsed-wave Doppler flow imaging.

The ultrasound pulse for therapy application is typically longer than that for imaging applications. Figure 8c shows the waveform used for LIFU therapy such as ultrasound-mediated BBB opening and ultrasonic neuromodulation. It should be noted that due to high acoustic attenuation in the skull, it may overheat even if LIFU is applied [82]. A continuous-wave is used for HIFU therapy as shown in Fig. 8d.

The typical ultrasound parameters including the acoustic intensities can be calculated based on the following two equations [15]:

$$I_{\text{sppa}} = 1/(T_0 \cdot \rho \cdot c) \cdot \int_0^{T_0} [P(t)]^2 \, \mathrm{d}t \tag{7}$$

$$I_{\text{spta}} = I_{\text{sppa}} \cdot T_1 \cdot T_3 / (T_2 \cdot T_4) \tag{8}$$

where $P(t)$ is the spatial peak instantaneous acoustic pressure, and T_0 is an integer representing the number of periods of the ultrasound waveform. The spatial peak pulse average intensity,

0885-3010 (c) 2020 IEEE. Personal use is permitted, but republication/redistribution requires IEEE permission. See http://www.ieee.org/publications_standards/publications/rights/index.html for more information.
Authorized licensed use limited to: Cornell University Library. Downloaded on September 01,2020 at 09:14:01 UTC from IEEE Xplore. Restrictions apply.

This article has been accepted for publication in a future issue of this journal, but has not been fully edited. Content may change prior to final publication. Citation information: DOI 10.1109/TUFFC.2020.3019932, IEEE Transactions on Ultrasonics, Ferroelectrics, and Frequency Control

i.e., I_{sppa} with units of W/cm^2, can be calculated by integrating the square of the instantaneous acoustic pressure over the time T_0 and then dividing the result by the mass density ρ and speed of sound c. The spatial peak temporal average intensity, i.e., I_{spta} with units of mW/cm^2 is calculated by multiplying I_{sppa} by T_1, T_2, T_3, and T_4, which represent the continuous pulse duration, pulse repetition period, sonication duration, and stimulus repetition period, respectively.

Equation 7 can be simplified for linear ultrasound waveform. A sinusoidal wave with the same amplitude of peak compression pressure and rarefaction pressure can be given as follows:

$$P(t) \approx P_0 \cdot \cos(2\pi \cdot f \cdot t) \tag{9}$$

where P_0 is the amplitudes of peak pressure, and f is the center frequency of the ultrasound waveform. The non-linearity can be negligible in LIFU and, therefore, I_{sppa} can be approximately calculated as:

$$I_{sppa} \approx P_0^2 / 2(\rho \cdot c) \tag{10}$$

The safety standard for brain ultrasound applications is guided by the Food and Drug Administration (FDA) guidelines for diagnostic ultrasound imaging devices. The mechanical risk of ultrasound is evaluated by the parameters I_{sppa} and the Mechanical Index (MI), while the thermal risk is evaluated by the parameters I_{spta} and Thermal Index (TI). The MI is given by:

$$MI = \frac{P_r}{\sqrt{f}} \tag{11}$$

where P_r is the peak rarefaction pressure (in MPa) and f is the center frequency (in MHz) of the ultrasonic waveform. The MI can predict the onset of inertial cavitation in the presence of microbubble.

According to the FDA guidelines for imaging applications in the adult brain, I_{sppa}, I_{spta}, and MI must not exceed 190 W/cm^2, 94 mW/cm^2, and 1.9, respectively [118]. These parameters are related to the ultrasonic pressure, ultrasonic frequency and pulse duration, and limiting these parameters is useful for decreasing the risk from thermal effects.

VII. Recently Developed Ultrasound Device and System for Brain Imaging and Therapy

Recent developments in ultrasound transducer and electronics along with imaging or therapeutic algorithms open new opportunities for brain diagnosis and therapy. Plane-wave based power Doppler using ultrafast imaging sequence can significantly improve the sensitivity of cerebral flow imaging [4]. Real-time 3D imaging can be achieved using a multiplane-wave scheme with a 1024-element 2D array transducer, which provides an imaging tool to track transient activities in the brain such as epileptiform events [119]. Transcranial 3D ultrasound imaging using 2D array transducer was proposed in [44, 45]. However, its imaging quality is relatively low and requires further development of skull compensation.

Figures 9a-b show an MRI compatible array transducer (ExAblate Neuro, InSightec Haifa). The transducer was used to induce a therapeutic effect in the brain through an intact skull

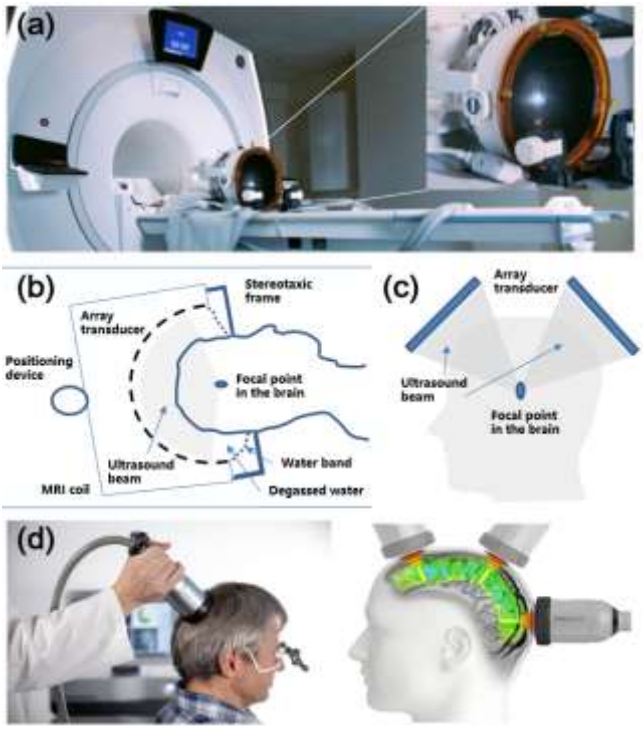

Fig. 9. The ultrasound transducer and system for brain therapy. (a) MRI guided array transducer for brain therapy. The images are from [120]. (b) The schematic of MRI guided ultrasound setup for brain therapy. (c) Multiple scalable array transducers for deep brain neuromodulation [121]. (d) Transcranial pulse stimulation handheld transducer for brain therapy [83]. The images in (d) are courtesy of Storz Medical AG.

[120]. It is a hemispheric-phased array with ~31cm diameter and ~15.5cm radius of curvature, which allows for ultrasound propagation through the entire skull. The operating frequency is 220 kHz (for BBB opening or neuromodulation) or 650 KHz (for thermal ablation). There are a total of 1024 elements in each transducer and each element can be controlled individually to enable focusing of the ultrasound beams in the brain. A stereotaxic frame is usually coupled with the transducer by fixing it to the patient's head under a local anesthetic [5]. Degassed water is also used as an acoustic coupling between the scalp and the transducer. Real-time MRI guidance increases the safety and accuracy of the treatment process [3]. A scalable 2D plane array transducer was proposed for brain neuromodulation, rendering a small size focal point and large steering range in the brain [121]. The transducer is MRI compatible and was used to carry out primate animal study *in vivo* for deep brain neuromodulation.

In addition, ultrasound-guided therapy was proposed. Dual-mode arrays were designed for image-guided therapy [13, 122], and multi-target neurostimulation or BBB opening can be achieved using array transducers [13, 106]. Moreover, multi-frequency array transducers were proposed for variable transmit focal sizes and multiple frequency excitation [102, 123]. Both half and second harmonic imaging can be obtained that are useful for cavitation detection and localization.

Portable ultrasound devices have been developed and evaluated on free-moving animals [15, 86] and humans [23, 83]. These devices can make the ultrasound treatment simple and convenient. The transducer can be attached directly to the head, and its location can be tracked in real-time using a 3D infrared camera technology. The therapeutic process is similar to the

0885-3010 (c) 2020 IEEE. Personal use is permitted, but republication/redistribution requires IEEE permission. See http://www.ieee.org/publications_standards/publications/rights/index.html for more information.
Authorized licensed use limited to: Cornell University Library. Downloaded on September 01,2020 at 09:14:01 UTC from IEEE Xplore. Restrictions apply.

This article has been accepted for publication in a future issue of this journal, but has not been fully edited. Content may change prior to final publication. Citation information: DOI 10.1109/TUFFC.2020.3019932, IEEE Transactions on Ultrasonics, Ferroelectrics, and Frequency Control

transcranial magnetic stimulation technology that can be well accepted by clinician.

Implantable ultrasound devices in the brain can offer a high-resolution localized BBB opening by avoiding the skull effect [124]. Once the device is implanted, the remaining process can be carried out easily. However, the main drawback of this method is the invasiveness of the procedure. It is expected that the new transducer designs and systems will promote the development and application of brain ultrasound. In particular, 3D acoustic lenses have been recently used to correct the aberrations induced by the human skull [125], with promising steering capabilities [126].

Ultrasonic neural dust, which is an ultrasound-based wireless neural recording technique has been applied to acquire the electrophysiological signal *in vivo* [127]. With this technique, ultrasound can not only provide a communication path between the neural cell and the outside console but also offer power supply for the mm-scale device implanted in the body [127, 128]. The recorded neural signal can be transmitted from the implanted device using ultrasonic backscatter. The ultrasound-based neural interface can have a great potential for brain-machine interface.

VIII. Conclusions

The ultrasound waves can penetrate non-invasively into brain tissues based on the different physical phenomena, enabling multiple clinical applications in diagnosis and therapy. Ultrasound has thus become a versatile and valuable tool in both preclinical and clinical studies that provides not only imaging information of the structure and function of the living brain but also enables manipulation of the brain and treatment of brain diseases. It is expected that ultrasound will play a major role in future clinical neurological studies.

IX. Acknowledgments

The authors would like to thank Dr Yongshuai Ge for providing the CT data and images, and Dr Yangzi Qiao for editing the MRI related contents in this paper. Both of them are affiliated with the Shenzhen Institutes of Advanced Technology, Chinese Academy of Sciences.

References

[1] K. J. Ressler and H. S. Mayberg, "Targeting abnormal neural circuits in mood and anxiety disorders: from the laboratory to the clinic," *Nature Neuroscience*, vol. 10, no. 9, pp. 1116-1124, Sep 2007.

[2] M. Tanter and M. Fink, "Ultrafast Imaging in Biomedical Ultrasound," *IEEE Transactions on Ultrasonics Ferroelectrics and Frequency Control*, vol. 61, no. 1, pp. 102-119, Jan 2014.

[3] K. Hynynen and R. M. Jones, "Image-guided ultrasound phased arrays are a disruptive technology for non- invasive therapy," *Physics in Medicine and Biology*, vol. 61, no. 17, pp. R206-R248, Sep 7 2016.

[4] E. Mace, G. Montaldo, B. F. Osmanski, I. Cohen, M. Fink, and M. Tanter, "Functional Ultrasound Imaging of the Brain: Theory and Basic Principles," *IEEE Transactions on Ultrasonics Ferroelectrics and Frequency Control*, vol. 60, no. 3, pp. 492-506, Mar 2013.

[5] N. Lipsman *et al.*, "Blood-brain barrier opening in Alzheimer's disease using MR-guided focused ultrasound," *Nature Communications*, vol. 9, Jul 25 2018, Art. no. 2336.

[6] A. Abrahao *et al.*, "First-in-human trial of blood-brain barrier opening in amyotrophic lateral sclerosis using MR-guided focused ultrasound," *Nature Communications*, vol. 10, Sep 26 2019, Art. no. 4373.

[7] S. Purkayastha and F. Sorond, "Transcranial Doppler ultrasound: technique and application," *Seminars in Neurology*, vol. 32, no. 4, pp. 411-420, Sep 2012.

[8] F. Bilotta, C. Robba, A. Santoro, R. Delfini, G. Rosa, and L. Agati, "Contrast-enhanced ultrasound imaging in detection of changes in cerebral perfusion," *Ultrasound in Medicine and Biology*, vol. 42, no. 11, pp. 2708-2716, Nov 2016.

[9] C. Demene *et al.*, "Functional ultrasound imaging of brain activity in human newborns," *Science Translational Medicine*, vol. 9, no. 411, Oct 2017, Art. no. eaah6756.

[10] X. T. Yin and K. Hynynen, "A numerical study of transcranial focused ultrasound beam propagation at low frequency," *Physics in Medicine and Biology*, vol. 50, no. 8, pp. 1821-1836, Apr 21 2005.

[11] G. Pinton, J.-F. Aubry, M. Fink, and M. Tanter, "Numerical prediction of frequency dependent 3D maps of mechanical index thresholds in ultrasonic brain therapy," *Medical Physics*, vol. 39, no. 1, pp. 455-467, Jan 2012.

[12] G. F. Li *et al.*, "Improved Anatomical Specificity of Non-invasive Neuro-stimulation by High Frequency (5 MHz) Ultrasound," *Scientific Reports*, vol. 6, Apr 2016, Art. no. 24738.

[13] G. Li *et al.*, "Imaging-Guided Dual-Target Neuromodulation of the Mouse Brain Using Array Ultrasound," *IEEE Transactions on Ultrasonics Ferroelectrics and Frequency Control*, vol. 65, no. 9, pp. 1583-1589, Sep 2018.

[14] Z. Cui *et al.*, "Enhanced neuronal activity in mouse motor cortex with microbubbles' oscillations by transcranial focused ultrasound stimulation," *Ultrasonics Sonochemistry*, vol. 59, Dec 2019, Art. no. 104745.

[15] G. Li *et al.*, "Noninvasive Ultrasonic Neuromodulation in Freely Moving Mice," *IEEE Transactions on Biomedical Engineering*, vol. 66, no. 1, pp. 217-224, Jan 2019.

[16] S. S. Yoo *et al.*, "Focused ultrasound modulates region-specific brain activity," *Neuroimage*, vol. 56, no. 3, pp. 1267-1275, Jun 2011.

[17] R. F. Dallapiazza *et al.*, "Noninvasive neuromodulation and thalamic mapping with low-intensity focused ultrasound," *Journal of Neurosurgery*, vol. 128, no. 3, pp. 875-884, Mar 2018.

[18] W. Lee *et al.*, "Image-guided focused ultrasound-mediated regional brain stimulation in sheep," *Ultrasound in Medicine and Biology*, vol. 42, no. 2, pp. 459-470, Feb 2016.

[19] T. Deffieux, Y. Younan, N. Wattiez, M. Tanter, P. Pouget, and J.-F. Aubry, "Low-Intensity Focused Ultrasound Modulates Monkey Visuomotor Behavior," *Current Biology*, vol. 23, no. 23, pp. 2430-2433, Dec 2 2013.

[20] L. Verhagen *et al.*, "Offline impact of transcranial focused ultrasound on cortical activation in primates," *Elife*, vol. 8, Feb 12 2019, Art. no. e40541.

[21] W. Legon *et al.*, "Transcranial focused ultrasound modulates the activity of primary somatosensory cortex in humans," *Nature Neuroscience*, vol. 17, no. 2, pp. 322-329, Feb 2014.

[22] H.-L. Liu *et al.*, "Design and experimental evaluation of a 256-channel dual-frequency ultrasound phased-array system for transcranial blood–brain barrier opening and brain drug delivery," *IEEE Transactions on Biomedical Engineering*, vol. 61, no. 4, pp. 1350-1360, 2014.

[23] A. N. Pouliopoulos *et al.*, "A Clinical System for Non-invasive Blood–Brain Barrier Opening Using a Neuronavigation-Guided Single-Element Focused Ultrasound Transducer," vol. 46, no. 1, pp. 73-89, 2020.

[24] S. Herculano-Houzel, "The human brain in numbers: a linearly scaled-up primate brain," *Frontiers in Human Neuroscience*, vol. 3, Nov 2009, Art. no. 31.

[25] G. Roth and U. Dicke, "Evolution of the brain and intelligence," *Trends in Cognitive Sciences*, Review vol. 9, no. 5, pp. 250-257, May 2005.

[26] J. DeFelipe, "The evolution of the brain, the human nature of cortical circuits, and intellectual creativity," *Frontiers in Neuroanatomy*, vol. 5, May 16 2011, Art. no. 29.

[27] H. Azhari, *Basics of biomedical ultrasound for engineers*. John Wiley & Sons, 2010.

[28] F. W. Kremkau, R. W. Barnes, and C. P. McGraw, "Ultrasonic attenuation and propagation speed in normal human brain," *Journal*

0885-3010 (c) 2020 IEEE. Personal use is permitted, but republication/redistribution requires IEEE permission. See http://www.ieee.org/publications_standards/publications/rights/index.html for more information.
Authorized licensed use limited to: Cornell University Library. Downloaded on September 01,2020 at 09:14:01 UTC from IEEE Xplore. Restrictions apply.

This article has been accepted for publication in a future issue of this journal, but has not been fully edited. Content may change prior to final publication. Citation information: DOI 10.1109/TUFFC.2020.3019932, IEEE Transactions on Ultrasonics, Ferroelectrics, and Frequency Control

of the Acoustical Society of America, vol. 70, no. 1, pp. 29-38, 1981 1981.

[29] H. Hori, G. Moretti, A. Rebora, and F. Crovato, "The Thickness of Human Scalp: Normal and Bald," *Journal of Investigative Dermatology*, vol. 58, no. 6, pp. 396-&, 1972.

[30] C. M. Moran, N. L. Bush, and J. C. Bamber, "Ultrasonic propagation properties of excised human skin," *Ultrasound in Medicine and Biology*, vol. 21, no. 9, pp. 1177-1190, 1995.

[31] S. B. Raymond and K. Hynynen, "Acoustic transmission losses and field alterations due to human scalp hair," *IEEE Transactions on Ultrasonics Ferroelectrics and Frequency Control*, vol. 52, no. 8, pp. 1415-1419, Aug 2005.

[32] M. D. Eames, A. Hananel, J. W. Snell, N. F. Kassell, and J.-F. Aubry, "Trans-cranial focused ultrasound without hair shaving: feasibility study in an ex vivo cadaver model," *Journal of therapeutic ultrasound*, vol. 1, pp. 24-24, 2013 2013.

[33] A. Adeloye, K. R. Kattan, and F. N. Silverman, "Thickness of the Normal Skull in the American Blacks and Whites," *American Journal of Physical Anthropology*, vol. 43, no. 1, pp. 23-30, 1975 1975.

[34] S. K. Law, "Thickness and resistivity variations over the upper surface of the human skull," *Brain topography*, vol. 6, no. 2, pp. 99-109, 1993 1993.

[35] G. Pinton, J. F. Aubry, E. Bossy, M. Muller, M. Pernot, and M. Tanter, "Attenuation, scattering, and absorption of ultrasound in the skull bone," *Medical Physics*, vol. 39, no. 1, pp. 299-307, Jan 2012.

[36] F. J. Fry and J. E. Barger, "Acoustical properties of the human skull," *Journal of the Acoustical Society of America*, vol. 63, no. 5, pp. 1576-1590, 1978 1978.

[37] F. Marquet *et al.*, "Non-invasive transcranial ultrasound therapy based on a 3D CT scan: protocol validation and in vitro results," *Physics in Medicine and Biology*, vol. 54, no. 9, pp. 2597-2613, May 7 2009.

[38] J. F. Aubry, M. Tanter, M. Pernot, J. L. Thomas, and M. Fink, "Experimental demonstration of noninvasive transskull adaptive focusing based on prior computed tomography scans," *Journal of the Acoustical Society of America*, vol. 113, no. 1, pp. 84-93, Jan 2003.

[39] G. W. Miller, M. Eames, J. Snell, and J.-F. Aubry, "Ultrashort echo-time MRI versus CT for skull aberration correction in MR-guided transcranial focused ultrasound: In vitro comparison on human calvaria," *Medical Physics*, vol. 42, no. 5, pp. 2223-2233, May 2015.

[40] T. Wang and Y. Jing, "Transcranial ultrasound imaging with speed of sound-based phase correction: a numerical study," *Physics in Medicine and Biology*, vol. 58, no. 19, pp. 6663-6681, Oct 7 2013.

[41] A. Wydra, E. Malyarenko, K. Shapoori, and R. G. Maev, "Development of a practical ultrasonic approach for simultaneous measurement of the thickness and the sound speed in human skull bones: a laboratory phantom study," *Physics in Medicine and Biology*, vol. 58, no. 4, pp. 1083-1102, Feb 21 2013.

[42] F. Vignon, J. F. Aubry, M. Tanter, A. Margourn, and M. Fink, "Adaptive focusing for transcranial ultrasound imaging using dual arrays," *Journal of the Acoustical Society of America*, vol. 120, no. 5, pp. 2737-2745, Nov 2006.

[43] J.-H. Kwon, J. S. Kim, D.-W. Kang, K.-S. Bae, and S. U. Kwon, "The thickness and texture of temporal bone in brain CT predict acoustic window failure of transcranial Doppler," *Journal of Neuroimaging*, vol. 16, no. 4, pp. 347-352, Oct 2006.

[44] B. D. Lindsey, E. D. Light, H. A. Nicoletto, E. R. Bennett, D. T. Laskowitz, and S. W. Smith, "The ultrasound brain helmet: new transducers and volume registration for in vivo simultaneous multi-transducer 3D transcranial imaging," *IEEE Transactions on Ultrasonics Ferroelectrics and Frequency Control*, vol. 58, no. 6, pp. 1189-1202, Jun 2011.

[45] B. D. Lindsey and S. W. Smith, "Pitch-catch phase aberration correction of multiple Isoplanatic Patches for 3D transcranial ultrasound imaging," *IEEE Transactions on Ultrasonics Ferroelectrics and Frequency Control*, vol. 60, no. 3, pp. 463-480, Mar 2013.

[46] S. W. Smith, K. Chu, S. F. Idriss, N. M. Ivancevich, E. D. Light, and P. D. Wolf, "Feasibility study: Real-time 3-D ultrasound imaging of the brain," *Ultrasound in Medicine and Biology*, vol. 30, no. 10, pp. 1365-1371, Oct 2004.

[47] N. M. Ivancevich, G. F. Pinton, H. A. Nicoletto, E. Bennett, D. T. Laskowitz, and S. W. Smith, "Real-time 3-D contrast-enhanced transcranial ultrasound and aberration correction," *Ultrasound in Medicine and Biology*, vol. 34, no. 9, pp. 1387-1395, Sep 2008.

[48] D. Phillips, S. Smith, O. Von Ramm, and F. Thurstone, "Sampled aperture techniques applied to B-mode echoencephalography," in *Acoustical holography*: Springer, 1975, pp. 103-120.

[49] J. F. Aubry, M. Tanter, J. Gerber, J. L. Thomas, and M. Fink, "Optimal focusing by spatio-temporal inverse filter. II. Experiments. Application to focusing through absorbing and reverberating media," *Journal of the Acoustical Society of America*, vol. 110, no. 1, pp. 48-58, Jul 2001.

[50] D. E. Soulioti, D. Espindola, P. A. Dayton, and G. Pinton, "Super-resolution imaging through the human skull," *IEEE transactions on ultrasonics, ferroelectrics, and frequency control*, vol. 67, no. 1, pp. 25-36, Jan 2020.

[51] M. A. O'Reilly and K. Hynynen, "A super-resolution ultrasound method for brain vascular mapping," *Medical Physics*, vol. 40, no. 11, Nov 2013, Art. no. 110701.

[52] S. A. Cummer, J. Christensen, and A. Alu, "Controlling sound with acoustic metamaterials," *Nature Reviews Materials*, vol. 1, no. 3, Mar 2016, Art. no. 16001.

[53] M. Fink, "Time reversal of ultrasonic fields. 1. basic principles," *IEEE Transactions on Ultrasonics Ferroelectrics and Frequency Control*, vol. 39, no. 5, pp. 555-566, Sep 1992.

[54] G. van Wezel-Meijler, S. J. Steggerda, and L. M. Leijser, "Cranial Ultrasonography in Neonates: Role and Limitations," *Seminars in Perinatology*, vol. 34, no. 1, pp. 28-38, Feb 2010.

[55] W. He *et al.*, "Intraoperative contrast-enhanced ultrasound for brain tumors," *Clinical Imaging*, vol. 32, no. 6, pp. 419-424, Nov-Dec 2008.

[56] D. Chauvet *et al.*, "In Vivo Measurement of Brain Tumor Elasticity Using Intraoperative Shear Wave Elastography," *Ultraschall in Der Medizin*, vol. 37, no. 6, pp. 584-590, Dec 2016.

[57] J. Xia *et al.*, "Evaluation of brain tumor in small animals using plane wave-based power doppler imaging " *Ultrasound in Medicine and Biology*, vol. 45, no. 3, pp. 811-822, Mar 2019.

[58] A. Dizeux *et al.*, "Functional ultrasound imaging of the brain reveals propagation of task-related brain activity in behaving primates," *Nature Communications*, vol. 10, Mar 28 2019, Art. no. 1400.

[59] A. Bergel, T. Deffieux, C. Demene, M. Tanter, and I. Cohen, "Local hippocampal fast gamma rhythms precede brain-wide hyperemic patterns during spontaneous rodent REM sleep," *Nature Communications*, vol. 9, Dec 18 2018, Art. no. 5364.

[60] C. Errico *et al.*, "Ultrafast ultrasound localization microscopy for deep super-resolution vascular imaging," *Nature*, vol. 527, no. 7579, pp. 499-+, Nov 26 2015.

[61] O. Couture, V. Hingot, B. Heiles, P. Muleki-Seya, and M. Tanter, "Ultrasound Localization Microscopy and Super-Resolution: A State of the Art," *IEEE Transactions on Ultrasonics Ferroelectrics and Frequency Control*, vol. 65, no. 8, pp. 1304-1320, Aug 2018.

[62] J. E. Kennedy, "High-intensity focused ultrasound in the treatment of solid tumours," *Nature Reviews Cancer*, vol. 5, no. 4, pp. 321-327, Apr 2005.

[63] D. Coluccia *et al.*, "First noninvasive thermal ablation of a brain tumor with MR-guided focused ultrasound," *Journal of therapeutic ultrasound*, vol. 2, pp. 17-17, 2014 2014.

[64] E. Martin, D. Jeanmonod, A. Morel, E. Zadicario, and B. Werner, "High-Intensity Focused Ultrasound for Noninvasive Functional Neurosurgery," *Annals of Neurology*, vol. 66, no. 6, pp. 858-861, Dec 2009.

[65] W. J. Elias *et al.*, "A pilot study of focused ultrasound thalamotomy for essential tremor," *New England Journal of Medicine*, vol. 369, no. 7, pp. 640-648, 2013.

[66] S. Moosa, R. Martinez-Fernandez, W. J. Elias, M. del Alamo, H. M. Eisenberg, and P. S. Fishman, "The role of high-intensity focused ultrasound as a symptomatic treatment for Parkinson's disease," *Movement Disorders*, vol. 34, no. 9, pp. 1243-1251, Sep 2019.

[67] W. J. Elias *et al.*, "A magnetic resonance imaging, histological, and dose modeling comparison of focused ultrasound, radiofrequency, and Gamma Knife radiosurgery lesions in swine thalamus Laboratory investigation," *Journal of Neurosurgery*, vol. 119, no. 2, pp. 307-317, Aug 2013.

[68] A. Pulkkinen, Y. Huang, J. Song, and K. Hynynen, "Simulations and measurements of transcranial low-frequency ultrasound therapy:

0885-3010 (c) 2020 IEEE. Personal use is permitted, but republication/redistribution requires IEEE permission. See http://www.ieee.org/publications_standards/publications/rights/index.html for more information.
Authorized licensed use limited to: Cornell University Library. Downloaded on September 01,2020 at 09:14:01 UTC from IEEE Xplore. Restrictions apply.

This article has been accepted for publication in a future issue of this journal, but has not been fully edited. Content may change prior to final publication. Citation information: DOI 10.1109/TUFFC.2020.3019932, IEEE Transactions on Ultrasonics, Ferroelectrics, and Frequency Control

skull-base heating and effective area of treatment," *Physics in Medicine and Biology*, vol. 56, no. 15, pp. 4661-4683, Aug 7 2011.

[69] Z. Xu *et al.*, "Intracranial inertial cavitation threshold and thermal ablation lesion creation using MRI-guided 220-kHz focused ultrasound surgery: preclinical investigation," *Journal of Neurosurgery*, vol. 122, no. 1, pp. 152-161, Jan 2015.

[70] N. McDannold, Y.-Z. Zhang, C. Power, F. Jolesz, and N. Vykhodtseva, "Nonthermal ablation with microbubble-enhanced focused ultrasound close to the optic tract without affecting nerve function Laboratory investigation," *Journal of Neurosurgery*, vol. 119, no. 5, pp. 1208-1220, Nov 2013.

[71] J. Song and K. Hynynen, "A 1372-element Large Scale Hemispherical Ultrasound Phased Array Transducer for Noninvasive Transcranial Therapy," in *8th International Symposium on Therapeutic Ultrasound*, vol. 1113, E. S. Ebbini, Ed. (AIP Conference Proceedings, 2009, pp. 377-381.

[72] D. Chauvet *et al.*, "Targeting accuracy of transcranial magnetic resonance-guided high-intensity focused ultrasound brain therapy: a fresh cadaver model Laboratory investigation," *Journal of Neurosurgery*, vol. 118, no. 5, pp. 1046-1052, May 2013.

[73] J. R. Sukovich *et al.*, "Targeted Lesion Generation Through the Skull Without Aberration Correction Using Histotripsy," *IEEE Transactions on Ultrasonics Ferroelectrics and Frequency Control*, vol. 63, no. 5, pp. 671-682, May 2016.

[74] V. K. T. Looi, C. Mougenot, K. Hynynen, J. Drake, "In vivo feasibiltiy study of boiling histotripsy with clinical sonalleve system in a neurological porcine model," *Program Booklet of the 16th International Symposium on Therapeutic Ultrasound*, pp. 64-66, 2016.

[75] J. R. Sukovich *et al.*, "In vivo histotripsy brain treatment," *Journal of Neurosurgery*, vol. 131, no. 4, pp. 1331-1338, Oct 2019.

[76] P. B. Rosnitskiy, B. A. Vysokanov, L. R. Gavrilov, O. A. Sapozhnikov, and V. A. Khokhlova, "Method for Designing Multielement Fully Populated Random Phased Arrays for Ultrasound Surgery Applications," *IEEE Transactions on Ultrasonics Ferroelectrics and Frequency Control*, vol. 65, no. 4, pp. 630-637, Apr 2018.

[77] P. B. Rosnitskiy, P. V. Yuldashev, O. A. Sapozhnikov, L. R. Gavrilov, and V. A. Khokhlova, "Simulation of nonlinear trans-skull focusing and formation of shocks in brain using a fully populated ultrasound array with aberration correction," *Journal of the Acoustical Society of America*, vol. 146, no. 3, pp. 1786-1798, Sep 2019.

[78] A. Carpentier *et al.*, "Clinical trial of blood-brain barrier disruption by pulsed ultrasound," *Science Translational Medicine*, vol. 8, no. 343, Jun 15 2016, Art. no. 343re2.

[79] G. Samiotaki and E. E. Konofagou, "Dependence of the Reversibility of Focused-Ultrasound-Induced Blood-Brain Barrier Opening on Pressure and Pulse Length In Vivo," *IEEE Transactions on Ultrasonics Ferroelectrics and Frequency Control*, vol. 60, no. 11, pp. 2257-2265, Nov 2013.

[80] J. Blackmore, S. Shrivastava, J. Sallet, C. R. Butler, and R. O. Cleveland, "Ultrasound neuromodulation: A review of results, mechanisms and safety," *Ultrasound in Medicine and Biology*, vol. 45, no. 7, pp. 1509-1536, Jul 2019.

[81] M. D. Menz *et al.*, "Radiation Force as a Physical Mechanism for Ultrasonic Neurostimulation of the Ex Vivo Retina," *Journal of Neuroscience*, vol. 39, no. 32, pp. 6251-6264, Aug 2019.

[82] C. Constans, P. Mateo, M. Tanter, and J.-F. Aubry, "Potential impact of thermal effects during ultrasonic neurostimulation: retrospective numerical estimation of temperature elevation in seven rodent setups," *Physics in Medicine and Biology*, vol. 63, no. 2, Jan 2018, Art. no. 025003.

[83] R. Beisteiner *et al.*, "Transcranial Pulse Stimulation with Ultrasound in Alzheimer's Disease-A New Navigated Focal Brain Therapy," *Advanced Science*, vol. 7, no. 3, Feb 2020.

[84] D. Folloni *et al.*, "Manipulation of Subcortical and Deep Cortical Activity in the Primate Brain Using Transcranial Focused Ultrasound Stimulation," *Neuron*, vol. 101, no. 6, pp. 1109-+, Mar 20 2019.

[85] N. Pang *et al.*, "Transcranial Ultrasound Stimulation of Hypothalamus in Aging Mice," *IEEE transactions on ultrasonics, ferroelectrics, and frequency control*, 2020-Jan-21 2020.

[86] W. Qiu *et al.*, "A Portable Ultrasound System for Non-Invasive Ultrasonic Neuro-Stimulation," *IEEE Transactions on Neural Systems and Rehabilitation Engineering*, vol. 25, no. 12, pp. 2509-2515, Dec 2017.

[87] H. Zhou *et al.*, "Wearable Ultrasound Improves Motor Function in an MPTP Mouse Model of Parkinson's Disease," *IEEE Transactions on Biomedical Engineering*, vol. 66, no. 11, pp. 3006-3013, Nov 2019.

[88] D. Zhang *et al.*, "Antidepressant-Like Effect of Low-Intensity Transcranial Ultrasound Stimulation," *IEEE Transactions on Biomedical Engineering*, vol. 66, no. 2, pp. 411-420, Feb 2019.

[89] X. Li, H. Yang, J. Yan, X. Wang, Y. Yuan, and X. Li, "Seizure control by low-intensity ultrasound in mice with temporal lobe epilepsy," *Epilepsy Research*, vol. 154, pp. 1-7, Aug 2019.

[90] Z. Zhang *et al.*, "Low-intensity ultrasound suppresses low-Mg2+-induced epileptiform discharges in juvenile mouse hippocampal slices," *Journal of Neural Engineering*, vol. 16, no. 3, Jun 2019, Art. no. 036006.

[91] S.-G. Chen *et al.*, "Transcranial focused ultrasound pulsation suppresses pentylenetetrazol induced epilepsy in vivo," *Brain Stimulation*, vol. 13, no. 1, pp. 35-46, Jan-Feb 2020.

[92] S. Ibsen, A. Tong, C. Schutt, S. Esener, and S. H. Chalasani, "Sonogenetics is a non-invasive approach to activating neurons in Caenorhabditis elegans," *Nature Communications*, vol. 6, Sep 2015, Art. no. 8264.

[93] A. V. Alexandrov *et al.*, "Ultrasound-enhanced systemic thrombolysis for acute ischemic stroke," *New England Journal of Medicine*, vol. 351, no. 21, pp. 2170-2178, Nov 2004.

[94] Y. K. Lu *et al.*, "Microbubble-Mediated Sonothrombolysis Improves Outcome After Thrombotic Microembolism-Induced Acute Ischemic Stroke," *Stroke*, vol. 47, no. 5, pp. 1344-1353, May 2016.

[95] M. Daffertshofer *et al.*, "Transcranial low-frequency ultrasound-mediated thrombolysis in brain ischemia - Increased risk of hemorrhage with combined ultrasound and tissue plasminogen activator - Results of a phase II clinical trial," *Stroke*, vol. 36, no. 7, pp. 1441-1446, Jul 2005.

[96] C. Baron, J. F. Aubry, M. Tanter, S. Meairs, and M. Fink, "Simulation of Intracranial Acoustic Fields in Clinical Trials of Sonothrombolysis," *Ultrasound in Medicine and Biology*, vol. 35, no. 7, pp. 1148-1158, Jul 2009.

[97] J. Depoorter, C. Dewagter, Y. Dedeene, C. Thomsen, F. Stahlberg, and E. Achten, "Noninvasive MRI thermometry with the proton resonance frequency (PRF) method: in vivo results in human muscle," *Magnetic Resonance in Medicine*, vol. 33, no. 1, pp. 74-81, Jan 1995.

[98] N. McDannold and S. E. Maier, "Magnetic resonance acoustic radiation force imaging," *Medical Physics*, vol. 35, no. 8, pp. 3748-3758, Aug 2008.

[99] Y. Hertzberg, A. Volovick, Y. Zur, Y. Medan, S. Vitek, and G. Navon, "Ultrasound focusing using magnetic resonance acoustic radiation force imaging: Application to ultrasound transcranial therapy," *Medical Physics*, vol. 37, no. 6, pp. 2934-2942, Jun 2010.

[100] L. Marsac *et al.*, "MR-guided adaptive focusing of therapeutic ultrasound beams in the human head," *Medical Physics*, vol. 39, no. 2, pp. 1141-1149, Feb 2012.

[101] V. Ozenne *et al.*, "MRI monitoring of temperature and displacement for transcranial focus ultrasound applications," *Neuroimage*, vol. 204, Jan 1 2020, Art. no. Unsp 116236.

[102] L. Deng, M. A. O'Reilly, R. M. Jones, R. An, and K. Hynynen, "A multi-frequency sparse hemispherical ultrasound phased array for microbubble-mediated transcranial therapy and simultaneous cavitation mapping," *Physics in Medicine and Biology*, vol. 61, no. 24, pp. 8476-8501, Dec 21 2016.

[103] S. Xu *et al.*, "Correlation Between Brain Tissue Damage and Inertial Cavitation Dose Quantified Using Passive Cavitation Imaging," *Ultrasound in Medicine and Biology*, vol. 45, no. 10, pp. 2758-2766, Oct 2019.

[104] G. Maimbourg, A. Houdouin, M. Santin, S. Lehericy, M. Tanter, and J.-F. Aubry, "Inside/outside the brain binary cavitation localization based on the lowpass filter effect of the skull on the harmonic content: a proof of concept study," *Physics in Medicine and Biology*, vol. 63, no. 13, Jul 2018, Art. no. 135012.

[105] M. Pan, Y. Zhang, Z. Deng, F. Yan, and G. Hong, "Noninvasive and Local Delivery of Adenoviral-Mediated Herpes Simplex Virus Thymidine Kinase to Treat Glioma Through Focused Ultrasound-Induced Blood-Brain Barrier Opening in Rats," *Journal*

0885-3010 (c) 2020 IEEE. Personal use is permitted, but republication/redistribution requires IEEE permission. See http://www.ieee.org/publications_standards/publications/rights/index.html for more information.
Authorized licensed use limited to: Cornell University Library. Downloaded on September 01,2020 at 09:14:01 UTC from IEEE Xplore. Restrictions apply.

This article has been accepted for publication in a future issue of this journal, but has not been fully edited. Content may change prior to final publication. Citation information: DOI 10.1109/TUFFC.2020.3019932, IEEE Transactions on Ultrasonics, Ferroelectrics, and Frequency Control

of Biomedical Nanotechnology, vol. 14, no. 12, pp. 2031-2041, Dec 2018.

[106] Z. Zhang *et al.*, "New Sm-PMN-PT Ceramic-based 2D Array for Low-intensity Ultrasound Therapy Application," *IEEE Transactions on Ultrasonics, Ferroelectrics, and Frequency Control*, vol. Accepted, 2020.

[107] K. K. Shung, *Diagnostic ultrasound: Imaging and blood flow measurements*. CRC press, 2015.

[108] C. C. Coussios, C. H. Farny, G. Ter Haar, and R. A. Roy, "Role of acoustic cavitation in the delivery and monitoring of cancer treatment by high-intensity focused ultrasound (HIFU)," *International Journal of Hyperthermia*, vol. 23, no. 2, pp. 105-120, Mar 2007.

[109] A. Dasgupta, M. Liu, T. Ojha, G. Storm, F. Kiessling, and T. Lammers, "Ultrasound-mediated drug delivery to the brain: principles, progress and prospects," *Drug discovery today. Technologies*, vol. 20, pp. 41-48, 2016-Jun 2016.

[110] I. Lentacker, S. C. De Smedt, and N. N. Sanders, "Drug loaded microbubble design for ultrasound triggered delivery," *Soft Matter*, vol. 5, no. 11, pp. 2161-2170, 2009.

[111] W. G. Pitt, G. A. Husseini, and B. J. Staples, "Ultrasonic drug delivery--a general review," *Expert opinion on drug delivery*, vol. 1, no. 1, pp. 37-56, 2004 2004.

[112] J. Ye *et al.*, "Ultrasonic Control of Neural Activity through Activation of the Mechanosensitive Channel MscL," *Nano Letters*, vol. 18, no. 7, pp. 4148-4155, Jul 2018.

[113] Z. Qiu *et al.*, "The Mechanosensitive Ion Channel Piezo1 Significantly Mediates In Vitro Ultrasonic Stimulation of Neurons," *iScience*, vol. 21, pp. 448-457, 2019.

[114] B. Krasovitski, V. Frenkel, S. Shoham, and E. Kimmel, "Intramembrane cavitation as a unifying mechanism for ultrasound-induced bioeffects," *Proceedings of the National Academy of Sciences of the United States of America*, vol. 108, no. 8, pp. 3258-3263, Feb 22 2011.

[115] M. Plaksin, S. Shoham, and E. Kimmel, "Intramembrane Cavitation as a Predictive Bio-Piezoelectric Mechanism for Ultrasonic Brain Stimulation," *Physical Review X*, vol. 4, no. 1, Jan 2014, Art. no. 011004.

[116] M. Wang and Y. Zhou, "Numerical investigation of the inertial cavitation threshold by dual-frequency excitation in the fluid and tissue," *Ultrasonics Sonochemistry*, vol. 42, pp. 327-338, Apr 2018.

[117] K. B. Bader, M. J. Gruber, and C. K. Holland, "Shaken and stirred: mechanisms of ultrasound-enhanced thrombolysis," *Ultrasound in Medicine and Biology*, vol. 41, no. 1, pp. 187-196, Jan 2015.

[118] "Marketing Clearance of Diagnostic Ultrasound Systems and Transducers, Guidance for Industry and Food and Drug Administration Staff," *Food and Drug Administration US, Docket Number: FDA-2017-D-5372*, https://www.fda.gov/regulatory-information/search-fda-guidance-documents/marketing-clearance-diagnostic-ultrasound-systems-and-transducers, Jun 2019.

[119] C. Rabut *et al.*, "4D functional ultrasound imaging of whole-brain activity in rodents," *Nature Methods*, vol. 16, no. 10, pp. 994-+, Oct 2019.

[120] A. Zafar *et al.*, "MRI-Guided High-Intensity Focused Ultrasound as an Emerging Therapy for Stroke: A Review," *Journal of Neuroimaging*, vol. 29, no. 1, pp. 5-13, Jan-Feb 2019.

[121] Y. Yang *et al.*, "Development of Scalable 2D Plane Array for Transcranial Ultrasonic Neuromodulation on Non-Human Primates: An Ex Vivo Study," *IEEE transactions on neural systems and rehabilitation engineering*, vol. 28, no. 2, pp. 361-369, 2020-Feb 2020.

[122] A. Haritonova, D. Liu, and E. S. Ebbini, "In vivo Application and Localization of Transcranial Focused Ultrasound Using Dual-Mode Ultrasound Arrays," *IEEE Transactions on Ultrasonics Ferroelectrics and Frequency Control*, vol. 62, no. 12, pp. 2031-2042, Dec 2015.

[123] C. Constans, T. Deffieux, P. Pouget, M. Tanter, and J. F. Aubry, "A 200-1380-kHz Quadrifrequency Focused Ultrasound Transducer for Neurostimulation in Rodents and Primates: Transcranial In Vitro Calibration and Numerical Study of the Influence of Skull Cavity," *IEEE Transactions on Ultrasonics Ferroelectrics and Frequency Control*, vol. 64, no. 4, pp. 717-724, Apr 2017.

[124] A. Carpentier *et al.*, "Clinical trial of blood-brain barrier disruption by pulsed ultrasound," *Science Translational Medicine*, vol. 8, no. 343, Jun 2016, Art. no. 343re2.

[125] G. Maimbourg, A. Houdouin, T. Deffieux, M. Tanter, and J. F. Aubry, "3D-printed adaptive acoustic lens as a disruptive technology for transcranial ultrasound therapy using single-element transducers," *Physics in Medicine and Biology*, vol. 63, no. 2, Jan 2018, Art. no. 025026.

[126] G. Maimbourg, A. Houdouin, T. Deffieux, M. Tanter, and J. F. Aubry, "Steering Capabilities of an Acoustic Lens for Transcranial Therapy: Numerical and Experimental Studies," *Ieee Transactions on Biomedical Engineering*, vol. 67, no. 1, pp. 27-37, Jan 2020.

[127] D. Seo *et al.*, "Wireless Recording in the Peripheral Nervous System with Ultrasonic Neural Dust," *Neuron*, vol. 91, no. 3, pp. 529-539, Aug 3 2016.

[128] D. Seo, J. M. Carmena, J. M. Rabaey, M. M. Maharbiz, and E. Alon, "Model validation of untethered, ultrasonic neural dust motes for cortical recording," *Journal of Neuroscience Methods*, vol. 244, pp. 114-122, Apr 15 2015.

Weibao Qiu was born in Yanbian, China. He received his B.S. degree from the Hefei University of Technology in 2004, and his M.S. degree from the State Key Laboratory of Precision Measurement Technology and Instruments, Tianjin University, China, in 2007. He obtained his Ph.D. degree from the Interdisciplinary Division of Biomedical Engineering, The Hong Kong Polytechnic University, in 2012. He is currently a professor at Shenzhen Institutes of Advanced Technology (SIAT), Chinese Academy of Sciences, and is the director of Shenzhen key laboratory of ultrasound imaging and therapy. He serves on the Technical Program Committee of IEEE International Ultrasonics Symposium (IUS), and is an Associate Editor of the IEEE Transactions on Ultrasonics, Ferroelectrics, and Frequency Control. His research interests are novel ultrasound transducer and system for biomedical imaging and therapy.

Ayache Bouakaz graduated received the MS degree in acoustics in 1992 and the Ph.D. degree in 1996 from the Department of Electrical Engineering at the Institut National des Sciences Appliqu ées de Lyon (INSA Lyon), France. In 1998, he joined the Department of Bioengineering at the Pennsylvania State University in State College, PA, USA as a postdoc for 2 years. From December 1999 to November 2004, he has been employed as an associate professor at the Erasmus University Medical Center, Rotterdam, The Netherlands. His research focused on imaging, ultrasound contrast agents and transducer design. Since 2009 he holds a permanent position as a director of research , he is the head of the Ultrasound and Imaging laboratory and is the deputy director of the iBrain institute. His research focuses on imaging and therapeutic applications of ultrasound. He was the general chair of the 2016 international conference IEEE IUS and he is the vice president of IEEE UFFC in charge of symposia.

0885-3010 (c) 2020 IEEE. Personal use is permitted, but republication/redistribution requires IEEE permission. See http://www.ieee.org/publications_standards/publications/rights/index.html for more information.
Authorized licensed use limited to: Cornell University Library. Downloaded on September 01,2020 at 09:14:01 UTC from IEEE Xplore. Restrictions apply.

This article has been accepted for publication in a future issue of this journal, but has not been fully edited. Content may change prior to final publication. Citation information: DOI 10.1109/TUFFC.2020.3019932, IEEE Transactions on Ultrasonics, Ferroelectrics, and Frequency Control

Elisa E. Konofagou is the Robert and Margaret Hariri Professor of Biomedical Engineering and Professor Radiology as well as Director of the Ultrasound and Elasticity Imaging Laboratory at Columbia University in New York City. Her main interests are in the development of novel elasticity imaging techniques and therapeutic ultrasound methods and more notably focused ultrasound in the brain for drug delivery and stimulation, myocardial elastography, electromechanical and pulse wave imaging, harmonic motion imaging with several clinical collaborations in the Columbia Presbyterian Medical Center and elsewhere. Elisa is an Elected Fellow of the American Institute of Biological and Medical Engineering, a member of the IEEE in Engineering in Medicine and Biology, IEEE in Ultrasonics, Ferroelectrics and Frequency Control Society, the Acoustical Society of America and the American Institute of Ultrasound in Medicine. She has co-authored over 200 published articles in the aforementioned fields. Prof. Konofagou is also a technical committee member of the Acoustical Society of America, the International Society of Therapeutic Ultrasound, the IEEE Engineering in Medicine and Biology conference (EMBC), the IEEE International Ultrasonics Symposium and the American Association of Physicists in Medicine (AAPM). Elisa serves as Associate Editor in the journals of IEEE Transactions in Ultrasonics, Ferroelectrics and Frequency Control, Ultrasonic Imaging and Medical Physics, and is recipient of awards such as the CAREER award by the National Science Foundation (NSF), the Nagy award by the National Institutes of Health (NIH) and the IEEE-EMBS Technological Achievement Award as well as additional recognition by the American Heart Association, the Acoustical Society of America, the American Institute of Ultrasound in Medicine, the Wallace H. Coulter foundation, the Bodossaki foundation, the Society of Photo-optical Instrumentation Engineers (SPIE) and the Radiological Society of North America (RSNA).

Hairong Zheng received the B.S. degree from the Harbin Institute of Technology, Harbin, China, in 2000, and the Ph.D. degree in mechanical engineering from the University of Colorado at Boulder, Boulder, CO, USA, in 2006. He joined the University of California Davis as a Post-Doctoral Fellow, and then became Project Scientist with the Biomedical Engineering Department. He is a Professor and the Vice Director with the Shenzhen Institutes of Advanced Technology (SIAT), Chinese Academy of Sciences, Shenzhen, China. He has authored or co-authored over 110 peer-reviewed journal papers and holds more than 40 patents, some of which have been translated to commercial products. He focuses on multifunction biomedical ultrasound including ultrasonic neuromodulation, and multimodality medical imaging systems. Dr. Zheng was a recipient of the National Outstanding Young Scientist Award of China (2013), the Tan Kah Kee Young Scientist Award of China (2014), and the National innovation award of China (2017). He is the Principle Investigator of Scientific Instruments Fund of NSFC for brain stimulation. He is an Associate Editor of the IEEE Transactions on Ultrasonics, Ferroelectrics, and Frequency Control. He serves on the Technical Program Committee of the IEEE International Ultrasonics Symposium.

0885-3010 (c) 2020 IEEE. Personal use is permitted, but republication/redistribution requires IEEE permission. See http://www.ieee.org/publications_standards/publications/rights/index.html for more information.
Authorized licensed use limited to: Cornell University Library. Downloaded on September 01,2020 at 09:14:01 UTC from IEEE Xplore. Restrictions apply.